CZECH TECHNICAL UNIVERSITY IN PRAGUE
FACULTY OF ELECTRICAL ENGINEERING

Diploma Thesis

Dispatcher support system for power balance control

Author: Ondřej Malík
Supervisor: Petr Havel

České vysoké učení technické v Praze
Fakulta elektrotechnická

Katedra řídicí techniky

ZADÁNÍ DIPLOMOVÉ PRÁCE

Student: **Ondřej Malík**

Studijní program: Elektrotechnika a informatika (magisterský), strukturovaný
Obor: Kybernetika a měření, blok KM1 - Řídicí technika

Název tématu: **Dispečerský systém pro řízení výkonové rovnováhy**

Pokyny pro vypracování:

1. Upravte stávající verzi algoritmu pro optimální pokrytí predikce systémové odchylky [1] tak, aby byly lépe zohledněny potřeby dispečera přenosové soustavy a technické možnosti provozu systému
2. Otestujte funkci systému na realistických datech
3. Vyzkoušejte možnost použití systému jako automatického regulátoru výkonové rovnováhy v přenosové soustavě

Seznam odborné literatury:

[1] Malík, O.: Predictive control of power balance in electric grid, bakalářská práce, ČVUT FEL, 2007

Vedoucí: Ing. Petr Havel

Platnost zadání: do konce letního semestru 2009/10

prof. Ing. Michael Šebek, DrSc.
vedoucí katedry

L.S.

doc. Ing. Boris Šimák, CSc.
děkan

V Praze dne 27. 2. 2009

Declaration

I declare that I have created my Diploma Thesis on my own and I have used only literature cited in the included reference list.

In Prague, _21. 5. 2009_

signature

Acknowledgement

Abstrakt

V této diplomové práci je představen koncept cenově optimálního řídicího systému výkonové rovnováhy v elektrizační soustavě. Na základě předpovědi vývoje výkonové rovnováhy je vypočítán rozvrh aktivace regulačních rezerv, který zajistí pokrytí výkonové nerovnováhy při minimálních nákladech na regulační energii. V pravidelných časových rozestupech je hledán nový rozvrh na základě aktualizované předpovědi výkonové rovnováhy a stavu regulačních rezerv, koncepčně je tedy systém podobný prediktivnímu řízení.

K formulaci optimalizačního problému je použito lineární programování s celočíselnými proměnnými a optimalizace je prováděna dostupnými výpočetními prostředky. Formulace umožňuje přesně modelovat dynamické vlastnosti regulačních rezerv (například zpoždění aktivace či rychlost změny výkonu) a dále umožňuje omezit aktivaci regulačních rezerv za pomoci dispečerských pravidel (například omezení frekvence aktivací či změn výkonu). Průběžná optimalizace je prováděna ve spojení s modelem centrálního PI regulátoru sekundární regulace.

Výsledky provedených testů ukazují, že navržený řídicí systém je schopen omezit náklady na regulační energii, aniž by byla snížena kvalita regulace, a může tedy být užitečný jako podpůrný prostředek pro rozhodování dispečerů při řízení výkonové rovnováhy v elektrizační soustavě.

Abstract

A concept of cost-optimal automatic controller for power balance control in a transmission system is proposed in this thesis. Based on prediction of future power balance development, the controller computes a schedule for activation of regulation reserves, which minimizes the regulation energy costs while maintaining required control performance. Such optimization is periodically repeated with updated power balance prediction and regulation reserves state, hence the concept is, to some extent, similar to model-based predictive controller (MPC).

The optimization problem is formulated as a mixed-integer linear program and optimized using available solvers. The formulation allows to precisely model the dynamics of regulation reserves (e. g. activation delays or ramping rates) and allows to impose dispatch constraints on their activation (e. g. activation change or power change limits). The optimization on a moving horizon is performed in conjunction with the PI controller model, which simulates the secondary frequency control actions.

The results of test cases show, that the proposed controller is capable of reducing the regulation energy costs without compromising the control performance. Therefore, the controller might prove useful in supporting the Transmission System Operator dispatchers decisions in power balance control.

Contents

List of Figures

List of Tables

Chapter 1

Introduction

The power balance control is an important control task required for stable and secure operation of the electric grid. In synchronously interconnected areas, such as the European Union for the Co-ordination of Transmission of Electricity (UCTE) a general control concept is centrally specified. In the UCTE, such concept is provided in the Operation Handbook [1], however, the way how the power balance is achieved differs in individual control areas. The entities responsible for the power balance control in the individual control areas are the Transmission System Operators (TSO), each of whom has specific rules and procedures to ensure the power balance (i. e. to keep the scheduled set-point of the foreign exchange with the neighbouring control areas). These procedures involve increasing or decreasing the power generation in a control area by activating the *regulation reserves*. The regulation reserves are most of the time activated by an automatic controller to compensate common power imbalances in the electric grid and in case of larger scale or long lasting power imbalances, the human dispatchers take control of the task.

Although the costs associated with regulation reserves activation are issued to the originators of the power imbalance, the TSO should minimize the costs in order to reduce unnecessary expenses for the power balance control. However, the activation of the regulation reserves in an economic manner is a complicated task for the human operator, since many factors have to be considered at one time, such as the expected open-loop area control error (ACE) development, energy prices and dynamic characteristics of the generation units or other properties, for example the capacity limitations or dispatch constraints.

In this thesis, a dispatcher support system capable of scheduling the activation of regulation reserves, which are currently controlled by the human operators, is presented.

The system will use a prediction of the open-loop ACE to find a cost-optimal schedule of regulation reserves activation while maintaining required control performance. Furthermore, the system will be utilized to perform periodic optimizations on a moving horizon, resulting in an automatic controller[1] with a concept, to some extent, similar to model-based predictive controller (MPC).

The proposed dispatcher support system is a follow-up to the thesis [2], where the basic ideas and regulation reserves dynamics models were presented. However, the formulation of the dynamics models either was not accurate enough or was too complex, resulting in poor control performance or low optimization speed. Moreover, some specifics of the power balance control were not considered, such as the activation of tertiary reserve in rising-price manner and the formulation did not deal with the initial conditions necessary for the function as an automatic controller on a moving horizon. In addition, the dispatch constraints were incorporated into the optimality criterion, thus requiring to tune several weights in the optimality criterion to achieve the required controller performance.

The current formulation attempts to address aforementioned shortcomings of the model in [2] and the problem is optimized on a moving horizon. The performance of the automatic controller is verified in series of test cases, in which the automatic controller is employed in place of human operators.

The basic principles of power balance control are given in chapter 2, the chapter 3 deals with the optimization problem formulation and the results of case-studies are presented in chapter 4.

---

[1]Since in all test cases the dispatch system is used to perform optimizations on a moving horizon, it will be further referred to as "automatic controller."

Chapter 2

Principles of power balance control

In order to maintain power balance in a control area in the UCTE, a control system consisting of automatic controllers as well as human operators is employed. A typical structure of such system is shown in figure 2.1.
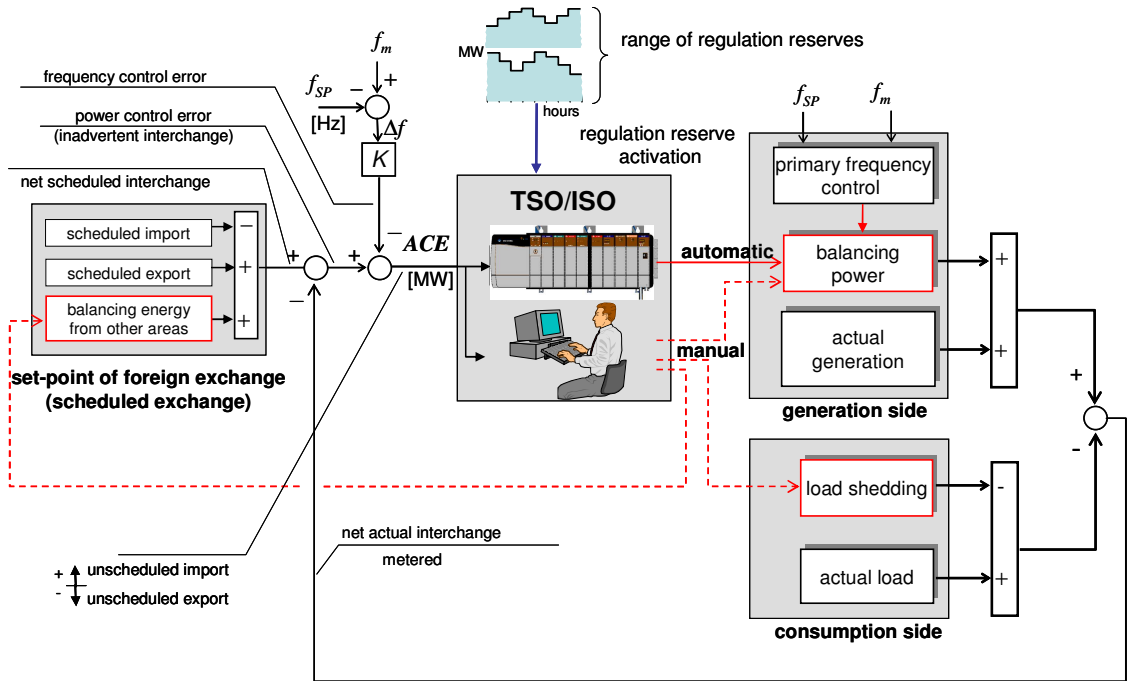
Figure 2.1: A typical structure of a control system for a control area in the UCTE

In [1], the UCTE defines three types of regulation reserves: *Primary frequency control*, *Secondary frequency control* and *Tertiary control*, which covers all other regulation

reserves used by the TSO. The Czech TSO, ČEPS, a. s. has defined and uses regulation reserves listed in table 2.1. Their features and typical usage patterns will be described in the following sections.

Response time	Regulation Reserve		
approx. 30 sec	**RZPR** (spinning)		primary reserve
max. 15 min	**RZ$_{15}$**	**RZQS** (non-spinning)	quick-start reserve (pumped-storage)
		RZSR (spinning)	secondary reserve
max. 30 min	**RZ$_{30}^+$** (positive)	**RZN$_{30}^+$** (non-spinning)	stand-by reserve
			load-shedding
			emergency assistance from abroad
		RZTR$^+$ (spinning)	tertiary spinning reserve
	RZ$_{30}^-$ (negative)	**RZN$_{30}^-$** (non-spinning)	emergency assistance from abroad
		RZTR$^-$ (spinning)	tertiary spinning reserve
more than 30 min	**RZN$_{>30}$** Replacement reserve	**RZDZ**	stand-by reserve
		Ereg	balancing energy

Table 2.1: Regulation reserves used by the Czech TSO

2.1 Primary frequency control

A purpose of the primary frequency control is to compensate fast fluctuations of the power balance (fluctuation of the frequency) in the entire synchronous interconnection (UCTE) and stabilize the entire system against contingencies such as outages of generation units. It is automatically activated by proportional controllers at each of the generation units

providing the service. Hence, the primary control is distributed across the interconnection and each control area contributes to this control with a power Δp_i^f according to a given frequency bias of the control area (called K-factor in the UCTE's terminology), K_i [MW/Hz],

$$\Delta p_i^f = K_i \Delta f, \tag{2.1}$$

where i denotes a particular control area and Δf is a frequency error (deviation of the measured frequency f_m from the frequency set-point $f_{SP} = 50$ Hz),

$$\Delta f = f_m - f_{SP}. \tag{2.2}$$

The K-factor can be viewed as a contribution coefficient, i.e., how much a particular area contributes to the joint action of the primary frequency control in the entire interconnected area.

2.2 Centrally controlled regulation reserves

Unlike the primary frequency control, remaining regulation reserves are controlled centrally from TSO's dispatch centre. These reserves are further divided into automatically controlled *Secondary frequency control* and *Tertiary control*, which is usually controlled manually. In figure 2.1, all centrally controlled domestic regulation reserves provided on generation side are represented by the block *balancing power*. The regulation reserves provided on the consumption side (*load shedding*) and regulation reserves from abroad (*balancing energy from other areas*) are also available at the hand of TSO's dispatchers.

2.2.1 Secondary frequency control

The purpose of the secondary frequency control is to keep foreign exchange with neighboring systems at a scheduled value (keep the power balance in the control area). It is provided on spinning generation units and activated by the central proportional-integral (PI) controller. The controller attempts to maintain the Area Control Error (ACE) at a zero value. ACE of a particular control area is defined as a difference between the scheduled and actual foreign power exchange (power control error), ΔP_i, corrected with

the effect of the primary control

$$ACE_i = \Delta P_i - \Delta P_i^f = \Delta P_i - K_i \Delta f. \tag{2.3}$$

The term ΔP_i^f, a frequency control error, compensates for the action of the distributed primary control within the area in order to avoid counter-regulation from the central secondary PI controller at the TSO's dispatch center. This ensures that the secondary control will only be called up in the control area which is the source of the disturbance (power imbalance).

2.2.2 Tertiary control

As was already mentioned, according to [1], the tertiary control encompasses all other regulation reserves different from primary and secondary control. With the Czech TSO, several types of regulation reserves are defined, which differ in reaction time, activation process and other properties as described in the following sections.

2.2.2.1 Quick-start reserve

In a typical usage pattern, the role of the quick start reserve is used to compensate for sudden power imbalances such as those caused by a failure of generation units. It is mostly provided on pumped-storage power stations. According to [3], the unit providing the quick-start reserve must be capable of providing its full power (or cease pumping) within 10 minutes of an activation command and keep it for at least 4 hours.

2.2.2.2 Tertiary spinning reserve

The tertiary spinning reserve is primarily used to free up the secondary regulation reserve and is of two types - the *positive* tertiary spinning reserve, which is used to increase the power output of the control area and the *negative* tertiary spinning reserve, which is used to decrease the power output. It is provided on spinning generation units. The full range of the tertiary reserve must be reached within a maximum of 30 minutes at a minimum rate of 2 MW/min. The activation of tertiary spinning reserve units is done strictly in rising-price manner, which is ensured by *criterial price coefficient* (CPC) as stated in [3].

2.2.2.3   Stand-by reserve

The stand-by reserves are typically activated in a case of a generation unit outage or a longer-lasting deficit of energy in the control area. It is usually provided on ready-to-start combined-cycle gas-turbine generation units. The generation unit providing the stand-by reserve must be capable of synchronization and reaching its full range within the agreed time (30, 60, 90 or 360 minutes). Usually, an activation delay is associated with the stand-by reserve unit startup as a result of necessary preparations before the unit is synchronized with the net.

2.2.2.4   Load shedding

Load shedding service is provided by entities at the demand-side, e.g. by an industrial enterprise which is ready to decrease its load upon request. However, this service is not so common and is very limited in the contracted volume.

2.2.2.5   Non-guaranteed regulation reserves

All previously mentioned regulation reserves were guaranteed, i. e. the contracts between the TSO and the providers exist that specify the time periods, when the regulation reserve must be available and may be activated upon the dispatchers request. In addition, a specific group of regulation reserves exists, which are not contracted in advance, but are obtained as needed. They are non-guaranteed as they might not be available in the case, when they are needed for the power balance control. The following non-guaranteed regulation reserves are used by the Czech TSO:

- *Emergency assistance from abroad* is based on mutual agreements with neighbouring TSO's.

- Purchase of *balancing energy* either on the domestic market or abroad. This service is available in time longer than 30 min, for foreign markets typically two hours, depending on availability of energy at the markets.

Chapter 3

Optimal dispatch of regulation reserves

In this chapter, first, a general concept of the proposed controller is given in section 3.1. The section 3.2 describes the main ideas of optimality criterion and constraints that model the dynamics of regulation reserves or limit their activation. This section may contain nonlinearities whenever it is believed that it makes the formulation more understandable. Finally, the section 3.3 presents the reformulation of section 3.2 as a mixed-integer linear program (MILP), which may be directly solved with available solvers.

3.1   Proposed control concept

The main part of the proposed controller is an optimization module that takes care of the cost-optimal activation of regulation reserves to minimize the closed-loop ACE (compensate the open-loop ACE). The optimization is performed over 6 hour horizon for which the open-loop ACE prediction can be found with acceptable accuracy. To capture the dynamics of the open-loop ACE and regulation reserves the sampling period was chosen to be 5 minutes.

Thus, each 5 minutes an updated open-loop ACE prediction is generated and the optimization is performed, i.e. an optimal schedule of reserves activation for the next 6 hours is found. Then, activation commands from the first time step are sent to generation units providing regulation reserves except for the units providing secondary reserve. Hence, the controller concept is to a certain extent similar to a model-based predictive

controller (MPC).

Not all types of regulation reserves are included in the optimization module, since they are either very limited in volume (load shedding) and thus negligible or their activation process may involve dispatchers participation (purchase of balancing energy on the market) and thus cannot be used in an automatic controller.

The PI controller works independently and compensates the remaining part of the open-loop ACE not compensated by the other regulation reserves (fast fluctuations in ACE and a prediction error). For this reason, to have a safety margin for prediction error and error caused by slower sampling, only a reduced range of the secondary reserve is included in the optimization module. For controller performance evaluation on historical data, a Simulink model of the secondary reserve central PI controller was used.

The optimization task was implemented in Yalmip [4] and the entire control concept was tested in Matlab [5] environment. To reduce the problem complexity and optimization time, the problem is formulated so that the sampling rate may be uneven along the optimization horizon. This allows for higher sampling rate at the beginning of the optimization horizon, where the open-loop ACE prediction is expected to be reasonably accurate, and lower sampling rate towards the end of the optimization horizon, where the prediction uncertainty increases.

3.2 General problem formulation

In this section optimality criterion (objective function) and constraints of the optimal dispatch task in implicit form will be formulated. In the following text, for simplicity, the term "unit" will denote a generation unit providing guaranteed regulation reserves that can be activated by the TSO's operator. Each such a unit labeled with an index i has its regulation range $\langle p_i^{\min}, p_i^{\max} \rangle$ [MW] provided to the TSO together with a given price C_i per MWh of supplied regulation energy and other technical parameters.

3.2.1 Basic variables

A state of each unit included in optimization is characterized by a set of variables. The basic variables, which are used in the formulation of most regulation reserves are listed in table 3.1.

Variable	Type	Description
$p_i(k)$	continuous	A power output of unit i in time sample k
$u_i(k)$	binary	An activation state of unit i in time sample k
$\Delta u_i(k)$	binary	An activation state change indicator
$\Delta u_i^{ON}(k)$	binary	A startup indicator
$\Delta u_i^{OFF}(k)$	binary	A shutdown indicator

Table 3.1: Basic variables used in the problem formulation

The term $p_i(k)$ is a current power output of a unit in time sample k [MW]. The variable $u_i(k)$ indicates, whether the unit is on or off in the sample k as follows

$$u_i(k) = \begin{cases} 1 \Leftrightarrow & \text{unit } i \text{ is on in time } k, \\ 0 \Leftrightarrow & \text{unit } i \text{ is off in time } k. \end{cases} \tag{3.1}$$

The variable $\Delta u_i(k)$ states, whether the unit activation state has changed in time sample k

$$\Delta u_i(k) = \begin{cases} 1 \Leftrightarrow & \text{activation or deactivation of unit } i \text{ in time } k \\ 0 & \text{otherwise.} \end{cases} \tag{3.2}$$

The meaning of the startup indicator $\Delta u_i^{ON}(k)$ is following

$$\Delta u_i^{ON}(k) = \begin{cases} 1 \Leftrightarrow & \text{activation of unit } i \text{ in time } k \\ 0 & \text{otherwise,} \end{cases} \tag{3.3}$$

and by analogy, the shutdown indicator $\Delta u_i^{OFF}(k)$ is defined as

$$\Delta u_i^{OFF}(k) = \begin{cases} 1 \Leftrightarrow & \text{deactivation of unit } i \text{ in time } k \\ 0 & \text{otherwise.} \end{cases} \tag{3.4}$$

3.2.2 Basic optimization horizon and units properties

The most important properties of the optimization horizon, which are used throughout this document, are the *number of samples in the optimization horizon N* and the *length of the time sample k, $T_s(k)$*.

The table 3.2 lists the most common units properties. If they present a time interval, such properties may become dependent on a time sample k as the time interval needs

to be converted into the equivalent number of samples with similar duration and due to the uneven time sampling of the optimization horizon, this number may not be constant over the whole optimization horizon. The discrete equivalents of these properties are also shown in the table 3.2. Likewise, the properties representing rates must be transformed to a change over the time sample length. If a property is not affected by a time sample length, only a discrete variable is given in the table 3.2.

Variable	Discrete equivalent	Description
-	$p_i^{max}(k)$	A maximal power output of a unit
-	$p_i^{min}(k)$	A minimal power output of a unit
Δp_i^{max}	$\Delta p_i^{max}(k)$	A maximal ramping rate
-	$C_i(k)$	A cost of 1 MWh of supplied energy
-	$C_i^{SU}(k)$	Startup costs of a unit
T_i^{SU}	$N_i^{SU}(k)$	A startup time of a unit
Td_i^{act}	$Nd_i^{act}(k)$	An activation delay of a unit
T^{int}	$N^{int}(k)$	A length of a time interval (e. g. an interval on which the number of activation changes is limited)

<div align="center">Table 3.2: Basic units properties</div>

In certain situations, the selected sampling of the optimization horizon might not allow to precisely convert a time interval into equivalent number of samples. In such cases, the equivalent number of samples is selected so that the sum of sample lengths is at least the length of the interval being converted. For example, if a 15-minute interval is to be converted and the optimization horizon is sampled with 10-minute sampling interval, two samples are selected as an equivalent number of samples, though the sum of their lengths is 20 minutes.

The maximal ramping rate is transfered to maximal power change between samples as follows

$$\Delta p_i^{\max}(k) = T_S(k) \cdot \frac{p_i^{\max}(k)}{T_i^{SU}}. \tag{3.5}$$

The transformation is based on a ramping rate, that would be achieved if the unit was ramping up from zero power output to its upper regulation range and the duration of such transition was exactly the startup time of a unit, T_i^{SU}. The resulting maximal power

change between samples is obtained by multiplying this ramping rate by the sample length $T_s(k)$.

3.2.3 Optimality criterion

To ensure that the automatic controller maintains the required power balance in the control area at minimal costs, the optimality criterion consists of two parts, energy costs and control performance penalization

$$J = J_{energy} + J_{control} \tag{3.6}$$

The energy costs J_{energy} are the costs of supplied regulation energy from all activated units and their startup costs

$$J_{energy} = \sum_i \sum_k \left[C_i\left(k\right) p_i\left(k\right) T_s\left(k\right) + c_i^{SU}\left(k\right) \right], \tag{3.7}$$

where the term $C_i\left(k\right) p_i\left(k\right) T_s\left(k\right)$ represents the costs of the energy supplied by the unit i during the time sample k. The startup costs of a unit $c_i^{SU}\left(k\right)$ are given by

$$c_i^{SU}\left(k\right) = C_i^{SU}\left(k\right) \Delta u_i^{ON}\left(k\right), \tag{3.8}$$

where $C_i^{SU}\left(k\right)$ denotes startup costs of the unit being activated.

The control performance penalization J_{ctrl} penalizes each MWh of the closed-loop ACE (uncompensated open-loop ACE)

$$J_{control} = \sum_{k=1}^{N} C_{ACE}\left(k\right) \cdot \left| \sum_i p_i\left(k\right) - ACE_o\left(k\right) \right| \cdot T_S(k), \tag{3.9}$$

where the term inside absolute value is the closed-loop ACE in sample k, $ACE_o(k)$ [MW] denotes the open-loop ACE prediction in sample k and $C_{ACE}(k)$ represents penalization price of uncompensated ACE. A standard linearization of the absolute value term according to [6] was used to keep the problem in linear form. A quadratic form of a control performance penalization was also considered in the form

$$J_{control} = \sum_{k=1}^{N} C_{ACE}^{QP}\left(k\right) \cdot \left(\sum_i p_i\left(k\right) - ACE_o\left(k\right) \right)^2 \cdot T_S(k), \tag{3.10}$$

where the term C_{ACE}^{QP} is a penalization coefficient, which allows to balance energy costs and control performance penalization. The problem with the optimality criterion in this form is directly solvable with a mixed-integer quadratic programming (MIQP) solver.

3.2.4 Regulation reserves models

The basic formulation principles of regulation reserves dynamics models will be presented in this section. The nonlinearities that appear in some equations will be later linearly reformulated in section 3.3. The problem constraints may be divided into two groups - dynamic characteristics of units and dispatch constraints. The dispatch constraints may be imposed on units, so that their activation conforms to standard usage patterns (e. g. minimal up and down times, activation frequency limits etc.). To ensure that the constraints will also be held between consecutive steps of optimization on a moving horizon, initial conditions must be correctly transferred from actual step to the following one.

3.2.4.1 Secondary frequency control

The secondary frequency control is modeled as a single unit whose power may be changed continuously within its regulation range. The power output changes between samples are limited by

$$-\Delta p_i^{\max}(k) \leq p_i(k+1) - p_i(k) \leq \Delta p_i^{\max}(k), \tag{3.11}$$

where the maximal power output change between samples $\Delta p_i^{\max}(k)$ is computed according to (3.5). To have a safety margin, the regulation range of the secondary reserve may be lowered by M_{SR}^{safety} [MW]

$$p_i^{\min}(k) + M_{SR}^{safety} \leq p_i(k) \leq p_i^{\max}(k) - M_{SR}^{safety}. \tag{3.12}$$

The only initial condition needed for the secondary frequency control model is the real power output at the time $k = 0$. If the initial power output is out of the reduced regulation range, it must be decreased to fit within the reduced regulation range to retain the problem feasibility.

3.2.4.2 Tertiary spinning reserve

Each unit of the tertiary spinning reserve is modeled individually, as available regulation range, dynamic characteristics and energy price of each unit vary in time, so if the tertiary reserve was modeled as a single unit, it would not be possible to model the overall dynamics precisely. The individual units providing tertiary spinning reserve are activated in "on/off" manner, meaning that once activated, the unit ramps up to its maximal power output with a constant ramping rate within a given startup time T_i^{SU}
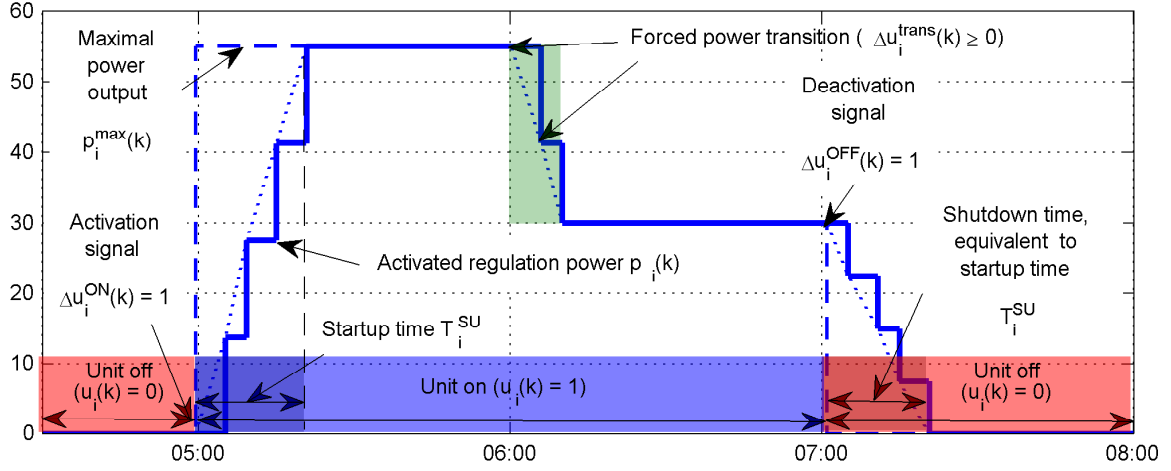
Figure 3.1: A tertiary spinning reserve unit activation example

and retains it until deactivation. If the available regulation range changes when the unit is on, the must perform a transition to the new maximal power output. A state of a tertiary unit is indicated by a binary variable $u_i(k)$, which is defined by (3.1). An example of a tertiary unit activation is given in figure 3.1.

To ensure the activation of the tertiary spinning reserve units in rising-price manner (as required by [3]), the positive tertiary reserve units activation state is controlled by an integer decision variable called Positive Criterial Price Coefficient (CPC^+) and by analogy, the negative tertiary reserve units are controlled by Negative Criterial Price Coefficient (CPC^-). If the CPC is higher than energy price of a unit, the unit is activated, and is deactivated as soon as the CPC is lowered under its energy price:

$$u_i(k) = \begin{cases} 1 \Leftrightarrow CPC(k) \geq C_i(k) \\ 0 \Leftrightarrow CPC(k) < C_i(k) \end{cases} \tag{3.13}$$

The equation (3.13) is valid for both, the positive and the negative tertiary spinning reserve (with CPC replaced by the respective Criterial Price Coefficient). Since the positive and negative tertiary spinning reserve is often provided on the same physical generation unit, it must be ensured that the positive and negative tertiary spinning reserve may not be activated at one time. For that purpose, a binary variables indicating the activation state of the tertiary spinning reserve u^{TR+} and u^{TR-} were introduced into the formulation. Their definition is following

$$u^{TR+}(k) = \begin{cases} 1 \Leftrightarrow & \text{at least one positive TR unit is on in time } k, \\ 0 \Leftrightarrow & \text{all positive TR units are off in time } k, \end{cases} \tag{3.14}$$

$$u^{TR-}(k) = \begin{cases} 1 \Leftrightarrow & \text{at least one negative TR unit is on in time } k, \\ 0 \Leftrightarrow & \text{all negative TR units are off in time } k, \end{cases} \qquad (3.15)$$

where TR stands for tertiary reserve. To ensure that the negative tertiary reserve is activated no sooner than all positive tertiary reserve units are off (and vice versa), the following constraints are included in formulation

$$u^{TR+}(k) = 1 \Rightarrow u^{TR-}(j) = 0, j \in k, \dots, k + N_{TR}^{SU}(k), \qquad (3.16)$$

$$u^{TR-}(k) = 1 \Rightarrow u^{TR+}(j) = 0, j \in k, \dots, k + N_{TR}^{SU}(k), \qquad (3.17)$$

where N_{TR}^{SU} is the number of samples equivalent to the tertiary reserve units startup time (which is considered to be the same for all tertiary reserve units). The constraint is applied at an interval $k, \dots, k + N_{TR}^{SU}$ because, as may be seen in figure 3.1, the activation indicator $u_i(k)$ is zero from the deactivation signal, though the power output of a unit is greater than zero for the following N_i^{SU} samples (during the unit shutdown process). Hence, these constraints assure, that the tertiary spinning reserve is not activated sooner than all units of the other tertiary spinning reserve type have their regulation reserve deactivated.

A frequency of the CPC changes may be user-limited to prevent undesired wear of the generation units, e.g. to "once in 20 min.", "three times in two hours" etc. (more of such constraints can be applied simultaneously). Binary CPC change indicators $\Delta CPC^{TR+}(k)$ and $\Delta CPC^{TR-}(k)$, defined as

$$\left| CPC^{TR+}(k) - CPC^{TR+}(k-1) \right| > 0 \Rightarrow \Delta CPC^{TR+}(k) = 1, \qquad (3.18)$$

$$\left| CPC^{TR-}(k) - CPC^{TR-}(k-1) \right| > 0 \Rightarrow \Delta CPC^{TR-}(k) = 1, \qquad (3.19)$$

are added into the problem formulation so that the CPC changes may be limited as follows

$$\sum_{k=j}^{j+N^{\text{int}}} \Delta CPC^{TR+}(k) \leq N, j = 0, \dots, N - N^{\text{int}}. \qquad (3.20)$$

The CPC^{TR-} changes limitation is formulated in similar way.

Behaviour of the unit transition between off and on state is modeled in following way: if the startup indicator $\Delta u_i^{ON}(k) = 1$, the unit increases the power output in following $N_i^{SU}(k)$ samples, where $N_i^{SU}(k)$ is an equivalent number of samples to a startup time of the unit. The transition from the on state back to the off state is modeled analogously, but initiated by the shutdown indicator Δu_i^{OFF}. Hence, the unit behaviour may be described

by

$$p_i (j + 1) = p_i (j) + \Delta p_i^{UP} (j) \Delta u_i^{ON} (k) - \Delta p_i^{DOWN} (j) \Delta u_i^{OFF} (k),$$
$$j \in k, \ldots, k + N_i^{SU} (k),$$
$$(3.21)$$

where $\Delta p_i^{UP} (j)$ and $\Delta p_i^{DOWN} (j)$ are the power output changes between the samples during the unit startup and shutdown. The way they are computed will be explained in detail in section 3.3.

The activation changes of individual units may also be limited similarly to (3.20)

$$\sum_{k=j}^{j+N_i^{int}} \Delta u_i (k) \leq N, j = 0, \ldots, N - N_i^{int}. \tag{3.22}$$

Such limitation may be desirable to avoid the unit deactivation before it reaches the full regulation range. This cannot be assured by the CPC limits alone, even when only single CPC change is allowed in the interval longer than the tertiary reserve units startup time, because the energy price of the unit varies in time, so its activation or deactivation may not be initiated by CPC change, but rather the unit energy price change.

To allow the unit to react on the maximal power output changes, the maximal power output of each tertiary reserve unit is modified before the optimization, so that in two consecutive samples, the change in the maximal power output does not exceed the limitation set by (3.5) (the power change limitation is computed from the greater of the maximal power outputs before and after the change). Example of such modification may be observed in figure 3.1, highlighted by a green box. If the unit has its regulation reserve fully activated in the time sample k when the maximal power output changes, a transition is allowed

$$p (k + 1) = p (k) + \Delta u_i^{trans} (k) \cdot [p_i^{max} (k + 1) - p_i^{max} (k)], \tag{3.23}$$

where the binary variable $\Delta u_i^{trans}(k)$ indicates, whether the power transition was performed. The $\Delta u_i^{trans}(k)$ is constrained to zero in all time samples, when no change in maximal power output occurs and also when the unit does not have the full range of its regulation reserve activated

$$\Delta u_i^{trans} (k) \begin{cases} \geq 0 \Leftrightarrow p_i (k) = p_i^{max} (k) \wedge |p_i^{max} (k + 1) - p_i^{max} (k)| > 0, \\ = 0 \text{ otherwise.} \end{cases} \tag{3.24}$$

If both conditions are met in certain sample, one of the two actions must be performed - the unit must either perform a transition to the new maximal power output or shut down, thus in such sample, the following must hold

$$\Delta u_i^{trans} (k) + \Delta u_i^{OFF} (k) = 1. \tag{3.25}$$

The initial conditions needed for the tertiary spinning reserve model are:

- The initial value of CPC in time $k = 0$ and a history of CPC changes for past T^{int} so that it may be considered in the constraint (3.20)

- For each unit, a history of activations Δu_i^{ON} and deactivations Δu_i^{ON} for past T^{int} to correctly implement the constraint (3.22)

If more CPC change limits or activation change limits are applied, then T^{int} should be the longest interval on which the limitation is imposed.

3.2.4.3   Stand-by reserve

The model of the stand-by reserve is, to certain extent, similar to the tertiary spinning reserve model. Each unit is modeled individually and is activated in an "on/off" manner. However, according to [3], once activated, the unit must be capable of providing the contracted regulation reserve for at least 36 hours, even if the contracted volume changes in the activation period, so the reaction to maximal power output changes is modeled in a different way to the tertiary reserve units. If the contracted volume changes during the unit activation, the unit retains its current power output until deactivation. In a subsequent activation, the unit ramps up to its currently contracted maximal power output. An example of such activation is shown in figure 3.2. The stand-by reserve dynamics may be defined by (3.21), where the power output change between samples during shutdown $\Delta p_i^{DOWN}(j)$ is computed differently to the tertiary reserve model, as will be described in section 3.3.

The frequency of unit activation is constrained by minimal up-time T_i^{minON}, minimal down-time T_i^{minOFF} and activation delay Td_i^{act}. Meaning of these user-defined parameters is illustrated in figure 3.2. The minimal up time T_i^{minON} is formulated as

$$\sum_{k=j}^{j+N_i^{\min ON}} \Delta u_i^{OFF}(k) \leq \left[1 - \Delta u_i^{ON}(k)\right], j = 0, \ldots, N - N_i^{\min ON}, \tag{3.26}$$

where $N_i^{\min ON}$ is a number of samples corresponding to the minimal up time T_i^{minON}. The constraint implies that Δu_i^{OFF} must be zero for $N_i^{\min ON}$ samples after unit activation. Analogously, the formulation of the minimal down time is

$$\sum_{k=j}^{j+N_i^{\min OFF}} \Delta u_i^{ON}(k) \leq \left[1 - \Delta u_i^{OFF}(k)\right], j = 0, \ldots, N - N_i^{\min OFF}. \tag{3.27}$$
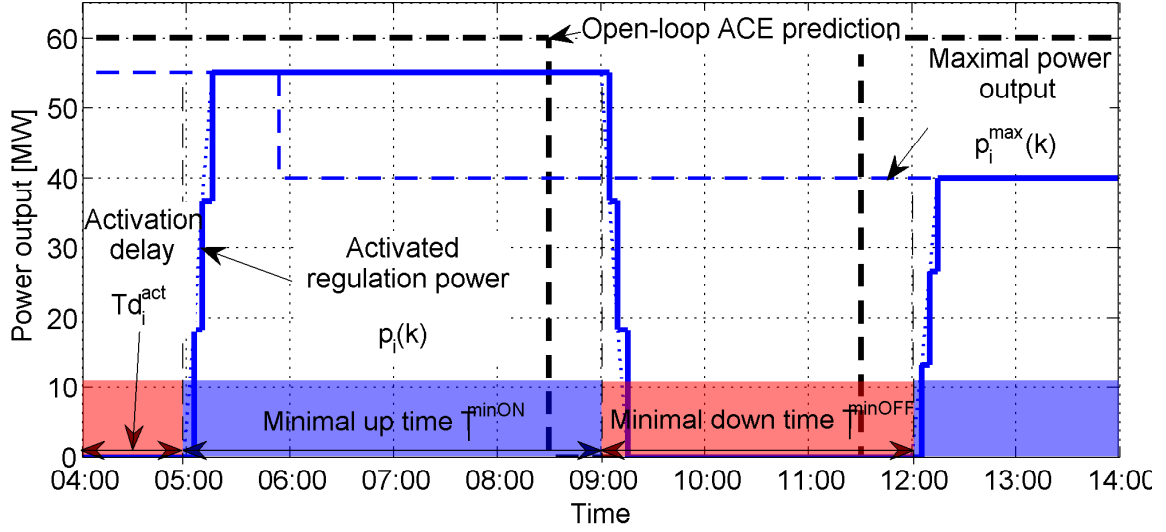
Figure 3.2: A stand-by reserve unit activation example

To ensure the activation delay Td_i^{act} at the beginning of the optimization horizon (first activation of a unit) a following constraint is applied

$$\Delta u_i^{ON}(k) = 0, \ k = 0, \ldots, Nd_i^{act}, \tag{3.28}$$

where Nd_i^{act} is number of samples corresponding to the activation delay. For other than the first activation, the activation delay Td_i^{act} is ensured by modifying the minimal down time to

$$T_i^{\min OFF} = \max\left(T_i^{\min OFF}, Td_i^{act}\right). \tag{3.29}$$

To define the initial state, only the time of last activation or deactivation is required, depending on which action was performed most recently.

3.2.4.4   Quick-start reserve

The quick-start reserve units are modeled individually. When a unit is on, the power output of the unit may continuously change within its regulation range

$$p_i^{\min}(k) \cdot u_i(k) \le p_i(k) \le p_i^{\max}(k) \cdot u_i(k), \tag{3.30}$$

where $u_i(k)$ is a binary variable defined in accordance with (3.1). An example of quick-start unit activation is given in figure 3.3. The grey zone indicates a power output range, to which the power output set-point may not be set.
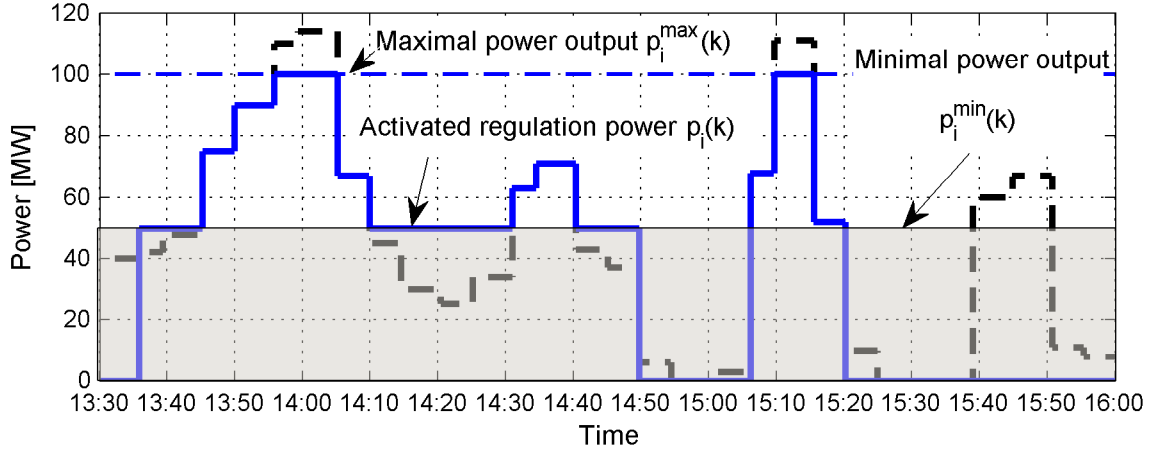
(a) No power change limitations, 1 activation in 60 minutes
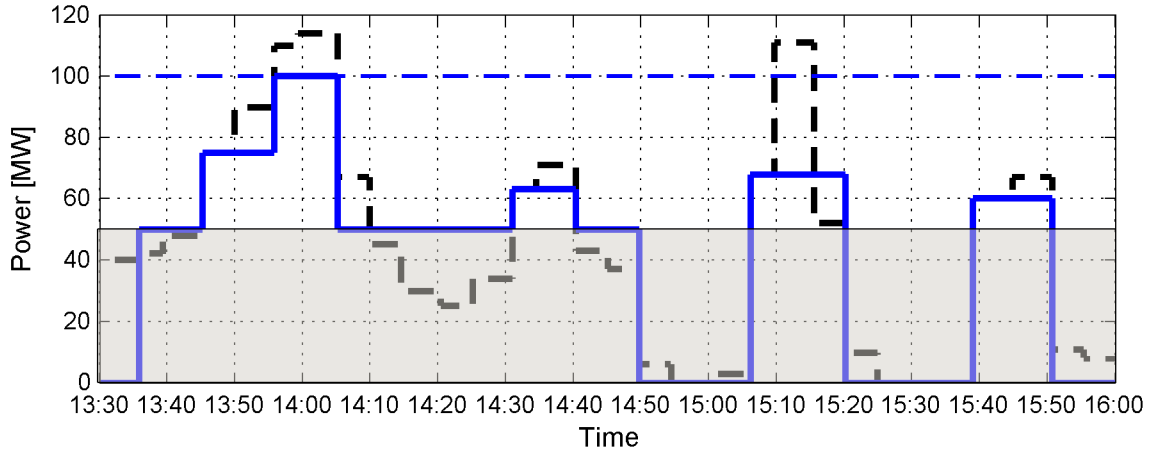
(b) 1 power change in 10 minutes, 3 activations in 60 minutes

Figure 3.3: A quick-start reserve unit properties and limitations example

As the startup time of quick-start units is usually lower than the sample time length, the maximal power output change between steps is not limited. To reflect the limited capacity of quick-start reserve units in the model, the capacity constraint is introduced into the formulation

$$\sum_{\forall k} T_s\left(k\right) \cdot p_i\left(k\right) \leq cap_i^{QS}, \tag{3.31}$$

where cap_i^{QS} is available capacity of the unit at the beginning of the optimization horizon in MWh. The available capacity is computed between the moving horizon steps to reflect the depleted or pumped energy. In the time, when the pumping process is engaged at the pumped-storage power plants, the only possible way to activate the quick-start reserve is to cease the pumping. Hence, in such time, the quick-start reserve at the unit may only

be deactivated (i. e. the pumping is in progress) or fully activated (i. e. the pumping is stopped), which is reflected in the problem formulation by the following constraint:

$$p_i(k) = b_i(k) \cdot p_i^{\max}(k), \tag{3.32}$$

where $b_i(k)$ is a binary variable, which ensures the activation to maximal power output or zero output.

The undesired wear prevention is controlled in two ways - a number of "cold starts" (i. e. the number of activations from off state) may be limited by adding a constraint similar to (3.22), but in which only startups are counted

$$\sum_{k=j}^{j+N_i^{\text{int}}} \Delta u_i^{ON}(k) \le N, j = 0, \dots, N - N_i^{\text{int}}. \tag{3.33}$$

Moreover, a constraint limiting the frequency of power output set-point changes may be also applied (e.g. to specify, that the power may change two times in 20 minutes), since the quick-start units are not designed for time-continuous control

$$\sum_{k=j}^{j+N^{\text{int}}} \Delta p_i^{ind}(k) \le N, j = 0, \dots, N - N^{\text{int}}, \tag{3.34}$$

where $\Delta p_i^{ind}(k)$ is a binary power output change indicator defined as

$$|p_i(k) - p_i(k-1)| > 0 \Rightarrow \Delta p_i^{ind}(k) = 1. \tag{3.35}$$

The effect of power output set-point change and activation limitations are illustrated in figure 3.3.

The initial state of the quick-start reserve units is described by:

- The initial power output in time $k = 0$

- The available capacity of the unit in time $k = 0$

- A history of activations Δu_i^{ON} for past N^{int} samples

- A history of power output set-point changes Δp_i^{ind} for past N^{int} samples

As with the initial conditions of the tertiary spinning reserve, if more power output set-point change limits or activation change limits are applied, then T^{int} should be the longest interval on which the limitation is imposed.

3.2.4.5   Emergency assistance from abroad

The emergency assistance from abroad is modeled as a single unit. Its power output set-point may be changed only in certain instants, so called "decision points", which are currently set to H:{00,15,30,45} (H represents an hour of a day). At the decision points, the power output set-point may be set to any value between the minimal power output $p_i^{min}(k)$ and maximal power output $p_i^{max}(k)$. The power output change is considered instant, as in reality it involves a change in foreign exchange set-point. Thus, a model of emergency assistance from abroad may be defined as

$$
\begin{aligned}
p_i^{\min}(k) \cdot u_i(k) \leq p_i(k) \leq p_i^{\max}(k) \cdot u_i(k) &\quad \Leftrightarrow k \in DP, \\
p_i(k) = p_i(k-1), u_i(k) = u_i(k-1) &\quad \Leftrightarrow k \notin DP,
\end{aligned}
\tag{3.36}
$$

where DP is a set of decision points. An example of emergency assistance from abroad activation is given in figure 3.4, with the decision points marked by the green dashed lines. If the selected sampling of the optimization horizon does not allow to set the decision points at H:{00,15,30,45}, the closest possible time samples are selected as the decision points. As certain time is needed to arrange the emergency assistance from abroad or to deactivate it, an activation delay Td_i^{act}, which prevents the unit activation or deactivation at the beginning of the optimization horizon, is included in the model

$$
\Delta u_i(k) = 0, \ k = 0, \dots, Nd_i^{act},
\tag{3.37}
$$

where Nd_i^{act} is a number of samples equivalent to the activation delay Td_i^{act}.
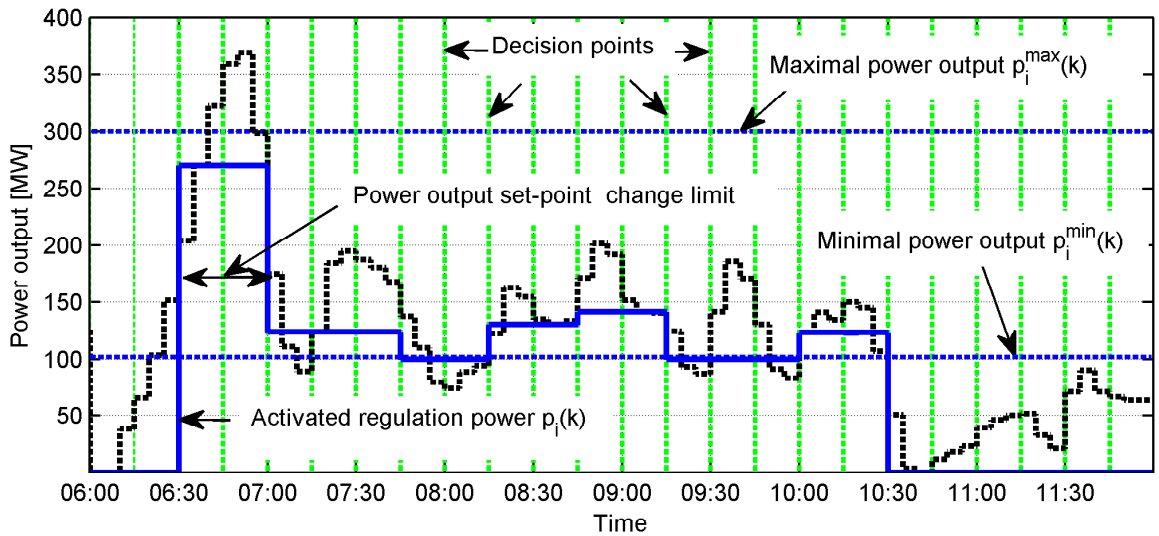

Figure 3.4: Emergency assistance from abroad activation example

The frequency of the emergency assistance from abroad power output set-point changes may be limited similarly to quick-start units by (3.34) and (3.35). The effect of such limitation is illustrated in figure 3.4, where the limit was set to one power output set-point change in 30 minutes.

The following initial conditions are needed for the model of emergency assistance from abroad:

- The initial power output in time $k = 0$

- A history of power output set-point changes Δp_i^{ind} for past N^{int} samples

3.3 Detailed problem formulation

In this section, details of the problem formulation will be presented. The relations between the basic binary optimization variables are given in section 3.3.1, the section 3.3.2 explains the initial conditions transfer between the consecutive steps of moving horizon optimization and in section 3.3.3 the nonlinearities in dynamics models of regulation reserves are linearly reformulated.

3.3.1 Optimization variables relations

Basically, there are two types of regulation reserves dynamics models in the formulation - the first type has an activation state $u_i(k)$ as a decision variable and with the second, the startup indicator $\Delta u_i^{ON}(k)$ and the shutdown indicator $\Delta u_i^{OFF}(k)$ act as decision variables.

For the dynamics models with activation state $u_i(k)$ as a decision variable, the startup indicator $\Delta u_i^{ON}(k)$ is derived as

$$\Delta u_i^{ON}(k) \geq u_i(k) - u_i(k-1), \tag{3.38}$$

and similarly, the shutdown indicator is computed as

$$\Delta u_i^{OFF}(k) \geq u_i(k-1) - u_i(k). \tag{3.39}$$

As opposed to (3.3) and (3.4), these constraints only guarantee, that the respective indicator is one when the change occurs, but do not imply that the indicator is zero

otherwise. However, since these indicators are further constrained in the dynamics models or are a part of the optimality criterion, it has no effect on the model functionality.

With the the startup indicator $\Delta u_i^{ON}(k)$ and the shutdown indicator $\Delta u_i^{OFF}(k)$ available, the activation change indicator $\Delta u_i(k)$ may be computed as a sum of these indicators

$$\Delta u_i(k) = \Delta u_i^{ON}(k) + \Delta u_i^{OFF}(k).\tag{3.40}$$

With models of regulation reserves dynamics, where the startup indicator $\Delta u_i^{ON}(k)$ and shutdown indicator $\Delta u_i^{OFF}(k)$ are the decision variables, the activation state change indicator $\Delta u_i(k)$ is also computed according to (3.40) and activation state $u_i(k)$ may be determined as

$$u_i(k) = u_i(k-1) + \Delta u_i^{ON}(k) - \Delta u_i^{OFF}(k).\tag{3.41}$$

In this type of dynamics models, the double sided implications in equations (3.2), (3.3) and (3.4) are held, which is important for the models of the tertiary reserve and stand-by reserve to work correctly.

3.3.2 Initial conditions details

As a result of actions performed in the past and unit dispatch constraints and dynamic characteristics, a part of the schedule at the beginning of the optimization horizon may become fixed, i. e. no change in unit activation state may be done in the preset time interval T_i^{preset} from the beginning of the optimization horizon.

For instance, with the stand-by reserve units, such situation arises anytime the unit is activated or deactivated due to the minimal up and down time constraints. If, for example, the activation of the unit is considered, the length of the interval on which the schedule is fixed T_i^{preset} depends on the minimal up time, activation delay and the time difference between the activation command and the start of the optimization horizon. The preset time interval is illustrated on stand-by reserve unit example in figure 3.5. Since the way, how the preset time interval T_i^{preset} is computed is specific to each regulation reserve dynamics model, it will be explained in sections 3.3.3.1 through 3.3.3.5.

After the T_i^{preset} is computed, it is converted into the equivalent number of samples N_i^{preset}. Using the N_i^{preset}, the power output of a unit $p_i(k)$ is fixed for samples $k = 0, \ldots, N_i^{preset}$ and the activation status $u_i(k)$ for samples $k = 0, \ldots, N_i^{preset} - 1$, which reflects the fact, that the first activation status change may be performed in sample
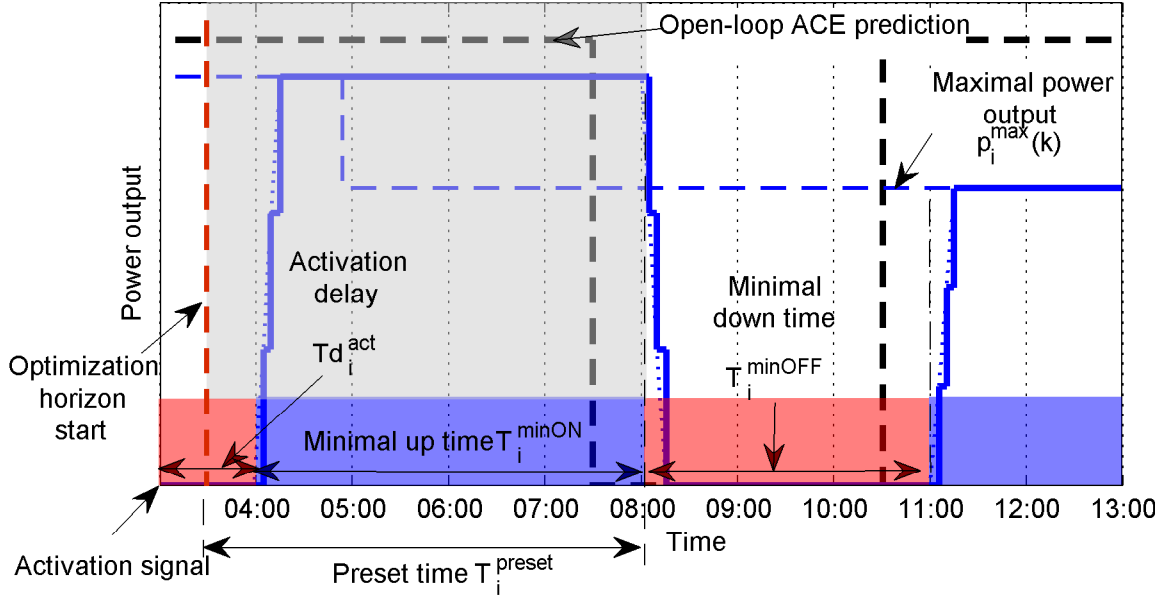
Figure 3.5: Example of schedule fixation at the beginning of the optimization horizon

$k = N_i^{preset}$. The fixation of $u_i(k)$ also fixes the activation change indicators $\Delta u_i(k)$, $\Delta u_i^{ON}(k)$ and $\Delta u_i^{OFF}(k)$ due to their relations to $u_i(k)$ as defined in section 3.3.1.

If change limits (activation changes, startup changes, power changes or CPC changes) are used to restrict the unit activation, then the influence of changes before the start of the optimization horizon is accounted for as in the following example.

A limitation of three activation changes in 60 minutes ($Nch_i^{60\,min} = 3$) and two changes performed in $t_1 = -30$ and $t_2 = -15$ minutes before the optimization horizon start are considered (the minus sign indicates that the time is before the optimization horizon start). It follows, that the change performed in t_1 influences the first 30 minutes of the optimization interval and the change in t_1 influences the first 45 minutes of the optimization interval. Thus, the interval $k = 0, \ldots, 30$ is influenced by both changes and interval $k = 30, \ldots, 45$ by one change. To reflect such influence, following constraints are imposed on the unit activation

$$\sum_{k=0}^{N^{30\,min}} \Delta u_i \leq Nch_i^{60\,min} - 2 = 1,$$

$$\sum_{k=N^{30\,min}}^{N^{45\,min}} \Delta u_i \leq Nch_i^{60\,min} - 1 = 2,$$

where $N^{30\min}$ and $N^{45\min}$ are equivalent number of samples to the 30-minute and 45-minute intervals starting at the beginning of the optimization horizon. If more change limits are used, the constraints are generated in similar way.

3.3.3 MILP reformulation of the regulation reserves dynamics models

3.3.3.1 Secondary frequency control

The secondary frequency control model contains no nonlinearities and equations (3.11) and (3.12) may be directly used in MILP problem.

Since no change limits, activation limits or startup delay are associated with the secondary frequency control and the power output may be changed continuously, the preset time interval T_i^{preset} is always zero. Hence, only the initial power output at $k = 0$ is required as an initial condition.

3.3.3.2 Tertiary spinning reserve

The model of the tertiary spinning reserve contains several nonlinearities that need to be reformulated in order to include them in mixed-integer linear program. The relation between the unit activation status $u_i(k)$ and the criterial price coefficient (3.13) is linearly formulated as

$$\frac{CPC^{TR+}(k) - C_i(k) + \varepsilon}{CPC_{\max}^{TR+}} \leq u_i(k) \leq \frac{CPC^{TR+}(k)}{C_i(k)}, \tag{3.42}$$

where CPC_{max}^{TR+} is a maximal energy price among all positive tertiary units across the optimization horizon. The formulation of such relation for negative tertiary reserve is analogous. If CPC is lower than the energy price of unit i in given sample k, the left hand side of (3.42) is negative and the right hand side is lower than one and greater then zero, constraining the $u_i(k)$ to zero. If CPC is greater than the energy price, the left hand side becomes positive, but lower than one, and the right hand side is greater than one, thus constraining the $u_i(k)$ to one. The term ε is a small constant $(0 < \varepsilon < 1)$ ensuring, that if the CPC equals the energy price, the $u_i(k)$ is constrained to one.

The constraint (3.42) is well defined only if the energy price of all units is greater than zero. In some rare cases, the energy price of negative tertiary reserve units may be lower than zero and the energy price of all negative tertiary reserve units must be increased by $-CPC_{min}^{TR-} + 1$ so that the energy price of all negative tertiary reserve units is greater

than zero. The term CPC_{min}^{TR-}, by analogy to CPC_{max}^{TR-}, is a minimal energy price among all negative tertiary units across the optimization horizon. The energy price is increased solely for the purpose of this constraint, the real energy prices are used in the optimality criterion.

The positive tertiary reserve activation state indicator (3.14) is linearly defined as

$$CPC_{min}^{TR+} \cdot u^{TR+}(k) \leq CPC^{TR+}(k) \leq CPC_{max}^{TR+} \cdot u^{TR+}(k). \tag{3.43}$$

The negative tertiary reserve activation state indicator (3.15) is formulated similarly. According to (3.43), whenever the CPC is lower than the price of the tertiary reserve unit with the lowest energy price, the tertiary reserve is considered as off.

The positive tertiary reserve activation change indicator (3.18) also needs to be linearly formulated, which is done in the following way:

$$\begin{aligned} \Delta CPC^{TR+}(k) &\geq \frac{CPC^{TR+}(k) - CPC^{TR+}(k-1)}{CPC_{max}^{TR+}}, \\ \Delta CPC^{TR+}(k) &\geq -\frac{CPC^{TR+}(k) - CPC^{TR+}(k-1)}{CPC_{max}^{TR+}}. \end{aligned} \tag{3.44}$$

Again, the negative tertiary reserve activation change indicator (3.19) is formulated analogously. As the constraint (3.20) is already linear, the linear reformulation of CPC change limits is complete.

The basic tertiary reserve units dynamics are defined by (3.21). The power output change between the samples during the unit startup $\Delta p_i^{UP}(j)$ is not constant due to the variable sample time length and is computed based on the maximal power output that the unit reaches after the startup is completed $p_i^{max}(k + N_i^{SU}(k))$

$$\begin{aligned} \Delta p_i^{UP}(j) &= T_S(j) \cdot \frac{p_i^{max}(k + N_i^{SU}(k))}{T_i^{SU}}, \\ j &\in k, \dots, k + N_i^{SU}(k) - 1. \end{aligned} \tag{3.45}$$

The shutdown of a unit is modeled in the same way, with the only difference being, that the output change between samples during shutdown $\Delta p_i^{DOWN}(j)$ is computed based on the maximal power at the beginning of the shutdown, $p_i^{max}(k)$:

$$\begin{aligned} \Delta p_i^{DOWN}(j) &= T_S(j) \cdot \frac{p_i^{max}(k)}{T_i^{SU}}, \\ j &\in k, \dots, k + N_i^{SU}(k) - 1. \end{aligned} \tag{3.46}$$

Since in some cases, the length of the equivalent time interval N_i^{SU} may not be equal to the unit startup time T_i^{SU} (especially at the points, where the sampling rate changes),

a modification of the power change between the last sample and the preceding one must be performed. Otherwise, the power output at the end of the startup would exceed the maximal power output as shown in figure 3.6. Hence, in such situation, the power output change between the last sample of startup and its predecessor is reduced, so that the final power output is exactly the maximal power output as follows:

$$\Delta p_i^{UP}\left(k + N_i^{SU}\left(k\right) - 1\right) = T_i^{SUrest}\left(k + N_i^{SU}\left(k\right) - 1\right) \cdot \frac{p_i^{\max}\left(k + N_i^{SU}\left(k\right)\right)}{T_i^{SU}}, \quad (3.47)$$

where the term $T_i^{SUrest}\left(k + N_i^{SU}\left(k\right) - 1\right)$ is the remaining time in the unit startup in the last sample before the startup is completed.
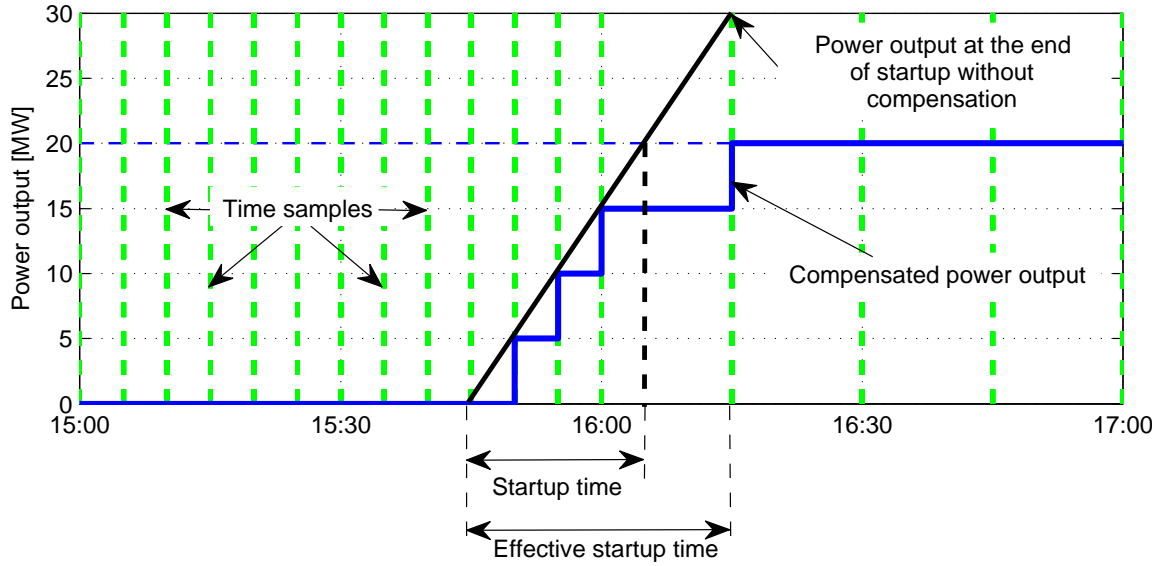

Figure 3.6: A unit startup modification to compensate the sampling rate change

The reaction to maximal power output changes that, as described by (3.23) is enforced by two constraints, which together present a linear form of constraints (3.24) and (3.25). Both are only generated for samples, in which the maximal power output actually changes, otherwise, the power transition indicator Δu_i^{trans} is constrained to zero. The first one bounds the Δu_i^{trans} to zero, whenever the unit is not fully activated:

$$\Delta u_i^{trans}\left(k\right) \leq \frac{p_i\left(k\right)}{p_i^{\max}\left(k\right)}. \quad (3.48)$$

The second one enforces the transition between adjacent maximal power output levels if the unit is fully activated and the maximal power output changes:

$$\frac{p_i\left(k\right) - p_i^{\max}\left(k\right) + \varepsilon}{p_i^{\max}\left(k\right)} \leq \Delta u_i^{trans}\left(k\right) + \Delta u_i^{OFF}\left(k\right) \leq 1, \quad (3.49)$$

where ε is a small constant, greater than the feasibility tolerance of a solver being used. The left hand side of the equation (3.49) is negative if the unit is not fully activated, thus is only states, that the transition between the two maximal power output levels and the unit deactivation may not happen at one time. If the unit is fully activated, the left hand side becomes positive, hence one of the two actions must be performed to satisfy the constraint.

To give a better insight into the tertiary reserve units dynamics constraint generation, an algorithm, which is used for such purpose, is presented:

1. Initialization

The power output change in each sample which is not preset by the initial conditions is initialized to zero:

$\Delta p_i(k) = 0, k \in N_i^{preset}, \dots, N$

2. Definition of standard power output changes

For $k = N_i^{preset} : N - 1$

    Compute the equivalent number of samples to the startup time $N_i^{SU}(k)$.

    For $j = k : k + N_i^{SU}(k) - 1$

        Compute the remaining startup time $T_i^{SUrest}(j)$.

        Compute the power output changes $\Delta p_i^{UP}(j)$ and $\Delta p_i^{DOWN}(j)$:

        If $T_i^{SUrest}(j) \geq T_S(j)$

$$\Delta p_i^{UP}(j) = T_S(j) \cdot \frac{p_i^{\max}\left(k + N_i^{SU}(k)\right)}{T_i^{SU}}$$

$$\Delta p_i^{DOWN}(j) = T_S(j) \cdot \frac{p_i^{\max}(k)}{T_i^{SU}}$$

        Else

            Compensate the power output change:

$$\Delta p_i^{UP}(j) = T_i^{SUrest}(j) \cdot \frac{p_i^{\max}\left(k + N_i^{SU}(k)\right)}{T_i^{SU}}$$

$$\Delta p_i^{DOWN}(j) = T_i^{SUrest}(j) \cdot \frac{p_i^{\max}(k)}{T_i^{SU}}$$

        End

        Add the power output changes to the total power change in given sample:

$$\Delta p_i(j) = \Delta p_i(j) + \Delta p_i^{UP}(j) \Delta u_i^{ON}(k) - \Delta p_i^{DOWN}(j) \Delta u_i^{OFF}(k)$$

    End

End

3. Definition of transitions between maximal power output levels

For $k = N_i^{preset} : N - 1$

    If $|p_i^{max}(k+1) - p_i^{max}(k)| > 0$

        Add the power output transition to the total power change in given sample:

        $\Delta p(k) = \Delta p(k) + \Delta u_i^{trans}(k) \cdot [p_i^{\max}(k+1) - p_i^{\max}(k)]$

        Apply the constraints (3.48) and (3.49).

    Else

        Constrain the $\Delta u_i^{trans}(k)$ to zero.

    End

End

4. Specification of relation between power output change $\Delta p_i(k)$ and the power output of a unit $p_i(k)$

For $k = N_i^{preset} : N - 1$

    $p_i(k+1) = p_i(k) + \Delta p_i(k)$

End

The number of samples at the beginning of the optimization horizon, during which the schedule is fixed, is for the individual units computed from the history of activation changes Δu_i and the unit startup time T_i^{SU}. The preset time interval T_i^{preset} is the time required for the unit to finish the startup or shutdown. The sufficient initial conditions for the model to work correctly are the activation state $u_i(N_i^{preset})$ and the power output $p_i(N_i^{preset})$ corresponding to this state - either a maximal power output or zero power output. It is also reasonable that the power output in the preset interval $k = 0, \ldots, N_i^{preset}$ is set to the expected startup or shutdown progress, so that the contribution of the unit to the power balance control in samples $k = 0, \ldots, N_i^{preset}$ is correct. Since the progress of startup or shutdown may be computed according to the dynamics model if the instant of activation or deactivation command is known, the history of Δu_i is sufficient as an initial condition as stated in section 3.2.4.2.

3.3.3.3   Stand-by reserve

Similarly to the tertiary spinning reserve, the basic stand-by reserve dynamics are defined by (3.21). The power output change between samples during the startup is also computed according to (3.45), however, due to the different behaviour when a change in maximal power output occurs, the power output change between samples during the shutdown

must be modified. As may be seen in the stand-by reserve unit activation example
(figure 3.2), when the shutdown is initiated, the unit power output may not be equal
to the current maximal power output. As a result, the unit shutdown must start at
the current power output of the unit, which implies, that the product of the continuous
variable $p_i(k)$ and binary variable Δu_i^{OFF} must be formulated. A MLD reformulation of
such product according to [7] was selected. Hence a new variable Δpu_i^{OFF}, which is equal
to the product of $p_i(k)$ and Δu_i^{OFF} is formulated as follows:

$$
\begin{aligned}
0 \leq \quad & \Delta pu_i^{OFF}(k) \leq p_i^{\max} \cdot \Delta u_i^{OFF} \\
p_i(k) - p_i^{\max} \cdot \left(1 - \Delta u_i^{OFF}\right) \leq \quad & \Delta pu_i^{OFF}(k) \leq p_i(k),
\end{aligned}
\tag{3.50}
$$

where $p_i^{\max}$ is a maximal power output of the unit across the whole optimization horizon.
With the product defined, the power output change during the shutdown may be rewritten
to

$$
\begin{aligned}
& \Delta p_i^{DOWN}(j) = T_{SM}(j) \cdot \frac{\Delta pu_i^{OFF}(k)}{T_i^{SU}}, \\
& j \in k, \ldots, k + N_i^{SU}(k).
\end{aligned}
\tag{3.51}
$$

Since the $\Delta p_i^{DOWN}(j)$ is no longer a constant, but is a variable and already includes the
effect of the shutdown indicator Δu_i^{OFF}, the unit dynamics are also modified to

$$
\begin{aligned}
& p_i(j+1) = p_i(j) + \Delta p_i^{UP}(j) \Delta u_i^{ON}(k) - \Delta p_i^{DOWN}(j), \\
& j \in k, \ldots, k + N_i^{SU}(k).
\end{aligned}
\tag{3.52}
$$

The algorithm, which generates the dispatch reserve dynamics model is similar to the
algorithm which is used for the tertiary reserve units, but the third step (reaction on
maximal power output changes) is omitted, since it is already included in basic dynamics.
The second step is modified to reflect the difference in Δp_i^{DOWN} computation and is shown
at the end of this section.

The preset time interval T_i^{preset} of stand-by reserve units is computed based on the last
activation or deactivation time (whichever happened the most recent). For this purpose,
the time of activations and deactivations is shifted by the activation delay Td_i^{act} into the
past to reflect the fact, that in order to activate or deactivate the unit, the activation
or deactivation signal must be sent in advance. If the unit was activated in the past,
the T_i^{preset} is such part of the time interval $Td_i^{act} + T_i^{minON}$ from the activation signal,
that overlaps with the optimization horizon as shown in figure 3.5. The situation is
analogous in case of deactivation of the unit in the past, but the interval $Td_i^{act} + T_i^{minOFF}$
is considered. Again, for the correct function of the stand-by reserve model, an activation
state at the end of the preset time interval $u_i(N_i^{preset})$ and an according power output

$p_i(N_i^{preset})$ (maximal power output or zero power output) is sufficient. The activation state $u_i(N_i^{preset})$ is implied by the most recent activation state change and the power output development may be computed from the stand-by reserve model if the time of the last activation state change is known, so the history of activations and deactivations is only needed to define the unit state at the beginning of the optimization horizon as stated in section 3.2.4.3.

The second step of the stand-by reserve dynamics generation algorithm is shown below:

2. Definition of standard power output changes

For $k = N_i^{preset} : N - 1$

    Compute the equivalent number of samples to the startup time $N_i^{SU}(k)$.

    For $j = k : k + N_i^{SU}(k) - 1$

        Compute the remaining startup time $T_i^{SUrest}(j)$.

        Compute the power output changes $\Delta p_i^{UP}(j)$ and $\Delta p_i^{DOWN}(j)$:

        If $T_i^{SUrest}(j) \geq T_S(j)$

$$\Delta p_i^{UP}(j) = T_S(j) \cdot \frac{p_i^{\max}\left(k + N_i^{SU}(k)\right)}{T_i^{SU}}$$

$$\Delta p_i^{DOWN}(j) = T_S(j) \cdot \frac{\Delta p u_i^{OFF}(k)}{T_i^{SU}}$$

        Else

            Compensate the power output change:

$$\Delta p_i^{UP}(j) = T_i^{SUrest}(j) \cdot \frac{p_i^{\max}\left(k + N_i^{SU}(k)\right)}{T_i^{SU}}$$

$$\Delta p_i^{DOWN}(j) = T_i^{SUrest}(j) \cdot \frac{\Delta p u_i^{OFF}(k)}{T_i^{SU}}$$

        End

        Add the power output changes to the total power change in given sample:

$$\Delta p_i(j) = \Delta p_i(j) + \Delta p_i^{UP}(j) \Delta u_i^{ON}(k) - \Delta p_i^{DOWN}(j)$$

    End

  End

3.3.3.4   Quick-start reserve

The only nonlinearity that must be dealt with in the model of quick-start reserve units as defined in section 3.2.4.4 is the power output change indicator Δp_i^{ind} definition (3.35).

This indicator is linearized in similar way as the CPC change indicator (3.44):

$$
\begin{aligned}
\Delta p_i^{ind}\left(k\right) &\geq \frac{p_i(k) - p_i(k-1)}{p_i^{\max}}, \\
\Delta p_i^{ind}\left(k\right) &\geq -\frac{p_i(k) - p_i(k-1)}{p_i^{\max}},
\end{aligned}
\tag{3.53}
$$

where $p_i^{\max}$ is a maximal power output of the unit in the optimization horizon.

As the quick-start units have no activation delay and the power output may be changed continuously, the number of preset samples N_i^{preset} is always zero, thus only the initial power at time $k = 0$ and an according activation state $u_i(0)$ must be set as an initial condition.

3.3.3.5   Emergency assistance from abroad

The model of the emergency assistance from abroad in section 3.2.4.5 is linear and may be directly included in mixed integer linear program. The length of the preset time interval T_i^{preset} is equal to the activation delay Td_i^{act}. The power output at the beginning of the optimization horizon $p_i(0)$ and an according activation state $u_i(0)$ are required as initial conditions and both are held unchanged for the first N_i^{preset} samples of the optimization horizon.

3.4   Optimization Problem Recapitulation

The resulting optimal dispatch problem is formulated as

$$\min_{CPC^{TR+},CPC^{TR-},u_i,\Delta u_i^{ON},\Delta u_i^{OFF},p_i} \left(J_{energy} + J_{control} \right) \tag{3.54}$$

subject to

(3.38) - (3.41),	(a)
(3.11), (3.12),	(b)
(3.20) - (3.23), (3.42) - (3.49),	(c)
(3.21), (3.26) - (3.29), (3.45), (3.50) - (3.52),	(d)
(3.30) - (3.34), (3.53),	(e)
(3.34), (3.36), (3.37), (3.53),	(f)

where

- the constraints (a) represent the relations between the basic decision variables,

- the decision variable p_i and constraints (b) are associated with the secondary frequency control model,

- the decision variables $CPC^{TR+}, CPC^{TR-}, \Delta u_i^{ON}, \Delta u_i^{OFF}$ and constraints (c) are associated with the tertiary spinning reserve model,

- the decision variables $\Delta u_i^{ON}, \Delta u_i^{OFF}$ and constraints (d) are associated with the stand-by reserve model,

- the decision variables p_i, u_i and constraints (e) are associated with the quick-start reserve model,

- the decision variables p_i, u_i and constraints (f) are associated with the emergency assistance from abroad model.

Chapter 4

Results

In this chapter, a performance of the proposed automatic controller will be evaluated. The section 4.1 analyses the controller actions in a short term view and focuses on prediction accuracy effects, influence of the secondary spinning reserve safety margin and also examines the results obtained with the quadratic form of control performance penalization. In section 4.2, a long term evaluation on a one-year interval is presented and compared to historical regulation reserves activation done by the TSO's dispatchers.

All test cases with the exception of the test cases focused on quadratic criterion control performance penalization, were optimized using the linear form of the optimality criterion 3.9 and the optimization horizon was sampled with 5-minute sampling interval for the first two hours and the rest of the optimization horizon was sampled with 30-minute sampling interval. On average, 30-50 units were included in the test cases and the problem solved in each step of the moving horizon optimization consisted of around 12000 variables (9500 binary, 2500 continuous) and 40000 constraints.

The optimization was carried out in Matlab environment [5] using the ILOG Cplex 11.0 [8] as a mixed-integer linear programming as well as mixed-integer quadratic programming solver. A comment on optimization speed is included in section 4.3.

4.1   Short term performance evaluation

To show the way, how the controller utilizes the regulation reserves, a set of short term test cases was carried out. Since the secondary frequency PI controller has a major influence on the resulting closed-loop ACE, in section 4.1.1, the historical records of the secondary

frequency PI controller actions are compared with the output of the model used in optimization. In section 4.1.2, influence of the secondary frequency control safety margin is illustrated and the margin to be used in long term test case is selected. The section 4.1.3 evaluates the controller performance with a quadratic form of an optimality criterion and with various settings of the control performance penalization coefficient C_{ACE}^{QP}. Finally, in section 4.1.4, three 24-hour optimization results examples are presented and the optimization with two types of open-loop ACE prediction is compared with the historical activation.

SR	Secondary frequency control
SR$^+$	Positive[2] secondary frequency control
SR$^-$	Negative[2] secondary frequency control
TR	Tertiary spinning reserve
TR$^+$	Positive tertiary spinning reserve
TR$^-$	Negative tertiary spinning reserve
QS	Quick-start reserve
SbR	Stand-by reserve
RA	Regulation energy from abroad
R$^+$	Remaining positive regulation reserves[3] (not included in optimization)
R$^-$	Remaining negative regulation reserves[4] (not included in optimization)
ACE	Closed-loop area control error
Costs	The total costs of the utilized regulation energy
RE	The total volume of the utilized regulation energy

Table 4.1: Symbols used in test case evaluation tables

The table 4.1 lists the abbreviations used in tables 4.2 to 4.6. These tables show the contribution of the different regulation reserve types to the total volume of utilized regulation energy (the total volume of utilized regulation energy is 100%). The two last columns in tables 4.2 to 4.6, ACE and Costs, present a comparison of closed-loop ACE and energy costs with historical activation (the closed-loop ACE and regulation energy costs in the historical records form the 100% value). All values are in percents.

---

[2]The term "positive" denotes the regulation energy, which is used to increase power generation in the control area (i. e. to lower the ACE) and the term "negative" denotes the regulation energy, which is used to decrease power generation in the control area (i. e. to increase the ACE).

[3]Purchase of positive balancing energy on the domestic market or abroad, load shedding.

[4]Purchase of negative balancing energy on the domestic market or abroad, generation shedding.

In the plots of historical activations in following sections, the control appears to have a step character; this is caused by the fact that only set-points are available in the historical records. The dashed lines represent available regulation ranges of individual services.

Since only aggregate power output of all units of the same regulation reserve type is available in historical records, the regulation energy costs of the tertiary spinning reserve, the stand-by reserve and the quick-start reserve were computed with assumption, that the individual units were activated strictly in rising-price manner. Hence, first, the units of the same regulation reserve type were ordered in rising-price manner. Then, in each time sample, the first N units were selected, where N is a number of units that were needed to be activated in order to reach the total power output of the regulation reserve. The resulting energy costs were determined based on the energy prices of the contributing units. The energy costs of the secondary frequency control and all regulation reserves, which were not included in optimization, were computed by simply multiplying the volume of utilized regulation energy and its price. In the optimization results, the energy costs were computed in the same way to minimize influence of the selected computation method.

As the emergency assistance from abroad was never activated in historical data record, nor was is activated in any optimization result, the emergency assistance from abroad is not included in evaluations.

### 4.1.1 Secondary frequency PI controller model evaluation

The secondary frequency control, due to its dynamic characteristics, is able to compensate even fast variations in open-loop ACE. Hence, in a situation, when the regulation range of the secondary frequency control is sufficient to compensate the open-loop ACE not compensated by the other regulation reserves, the secondary PI controller dynamics are the leading factor, which influences the resulting closed-loop ACE. An updated version of the secondary frequency PI controller model presented in [9] was employed in moving horizon simulations. To judge the selected model influence on the resulting ACE in the test cases, figure 4.1 compares the model performance to the real secondary frequency PI controller on two selected intervals.

The figure 4.1(a) allows to compare the dynamics in a typical situation with no measurement errors in historical data. The difference between the model and the real PI controller output is minimal, although the dynamics of the PI controller model are slightly faster. The figure 4.1(b) shows a situation, when the real PI controller did not precisely

track open-loop ACE development, resulting in a substantial increase in closed-loop ACE. Such a behaviour may be attributed to a measurement error or results from the way the secondary frequency control power output is determined from measurements at generation units.
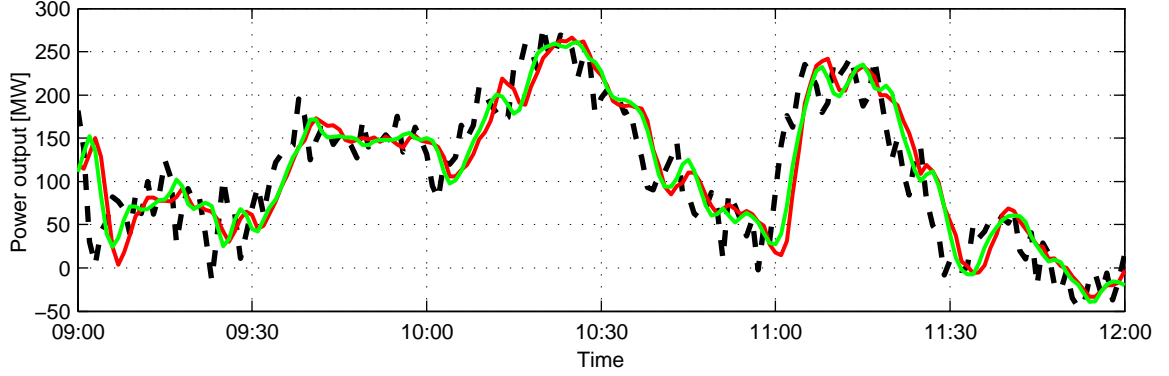

(a) No measurement error
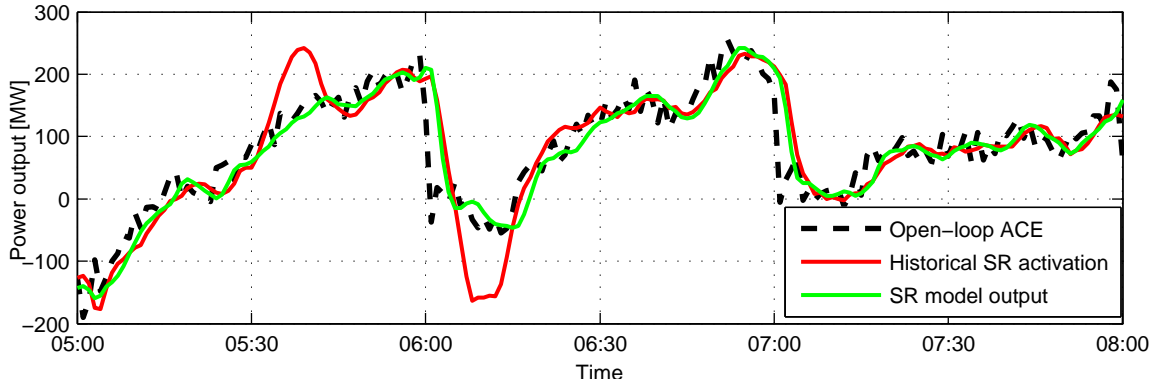
(b) With measurement error

Figure 4.1: Comparison of the secondary reserve model with historical records

4.1.2 Secondary reserve safety margin influence

The main reason for reducing the secondary frequency control regulation range by a safety margin is to have a reserve for compensation of prediction inaccuracy and errors resulting from the sampling of the optimization horizon. The effect the safety margin M_{SR}^{safety} may be observed in figures 4.2(b) to 4.2(d) and the schedule is also compared to historical regulation reserves utilization shown in 4.2(a).

The distribution of regulation energy among the regulation reserves is presented in table 4.2. The closed-loop ACE is only slightly increased when no safety margin was
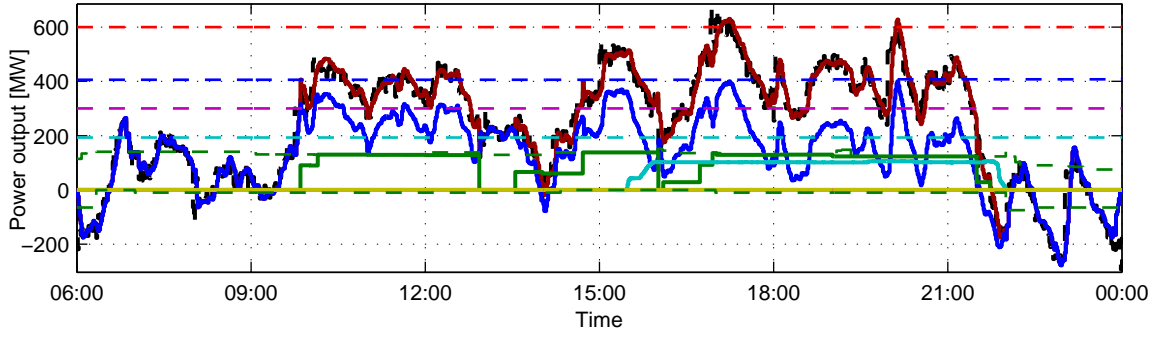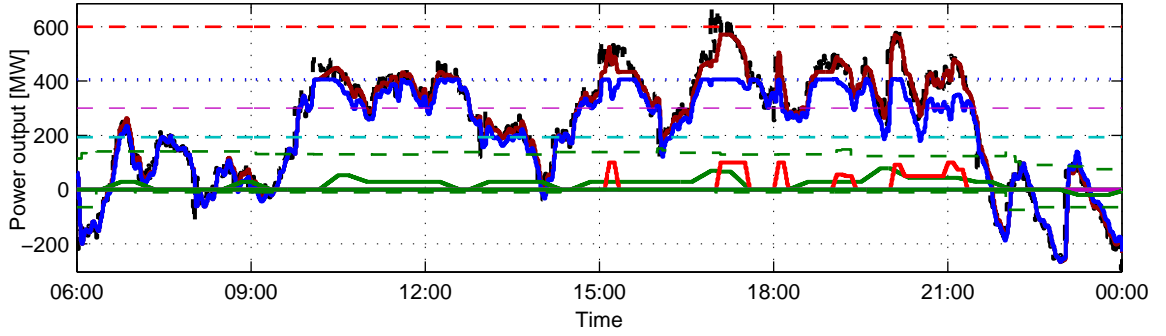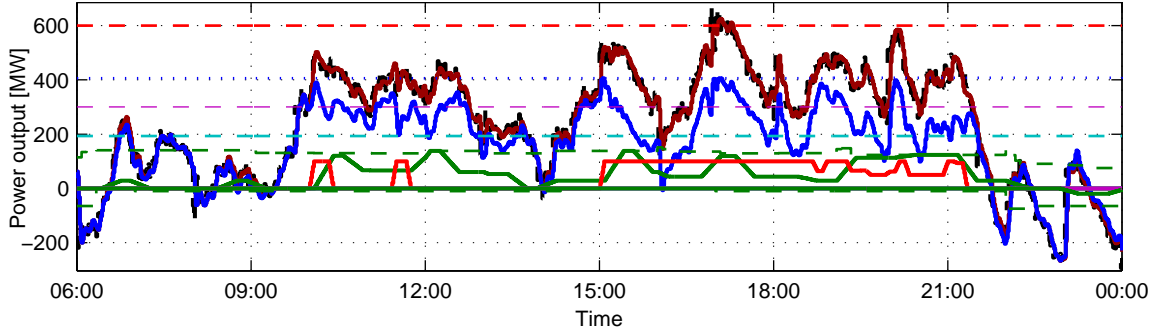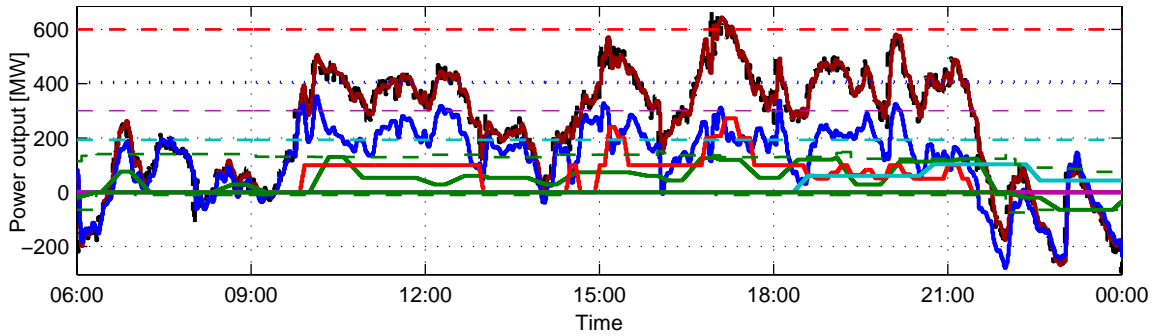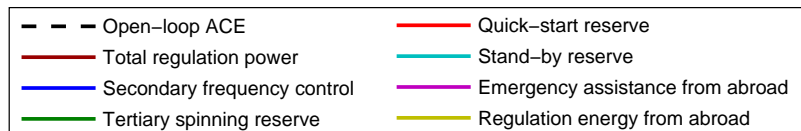
(a) Historical activation

(b) Optimization result with safety margin $M_{SR}^{safety} = 0$ MW

(c) Optimization result with safety margin $M_{SR}^{safety} = 100$ MW

(d) Optimization result with safety margin $M_{SR}^{safety} = 200$ MW

− − − Open−loop ACE	Quick−start reserve
Total regulation power	Stand−by reserve
Secondary frequency control	Emergency assistance from abroad
Tertiary spinning reserve	Regulation energy from abroad

Figure 4.2: Example of the secondary reserve safety margin influence

used (figure 4.2(b)), but the secondary frequency control was frequently used up to its limits and contributed with 88% to the total volume of the utilized regulation energy. Since energy price of the secondary frequency control is low, the total regulation energy costs are the lowest with no safety margin, but such setting leaves very little space for compensation if the prediction error was higher. Even with safety margin set at 100 MW, the secondary frequency control occasionally reaches its upper regulation range limit. This is eliminated at 200 MW setting, however, it also leads to a significant energy costs increase, since more expensive regulation reserves were utilized.

	Relative regulation energy utilization [%]								ACE	Costs
	SR			TR			QS	SbR		
	Tot.	SR$^+$	SR$^-$	Tot.	TR$^+$	TR$^-$				
History	61.7	55.6	6.1	25.4	25.4	0	0	12.9	100	100
Margin 0 MW	88.0	82.2	5.8	8.2	7.8	0.4	3.8	0	92.5	82.9
Margin 100 MW	69.9	64.1	5.8	17.8	17.5	0.3	12.3	0	89.2	89.7
Margin 200 MW	53.5	46.7	6.8	19.7	17.9	1.8	19.5	7.4	90.2	99.6

Table 4.2: Safety margin influence example - regulation energy utilization

The safety margin of 100 MW was selected for the automatic controller long term test case, since it presents a reasonable compromise between control performance and regulation energy costs.

4.1.3 Quadratic criterion penalization coefficient influence

With the linear form of the optimality criterion, the control performance penalization may only set the maximal energy price of the units that are to be included in the optimization. On the other hand, the quadratic form of the control performance penalization provides a method for finer balancing of control performance and energy costs. Due to the progressive penalization when the quadratic form is used, small values of closed-loop ACE are tolerated and high values should be suppressed. By varying the penalization coefficient C_{ACE}^{QP}, the strictness of the controller may be influenced as illustrated in figures 4.3(b) to 4.3(d). For reference, historical activation is also presented in figure 4.3(a) and the distribution of regulation energy among the regulation reserves is given in table 4.3 along with closed loop ACE and regulation energy costs comparison.
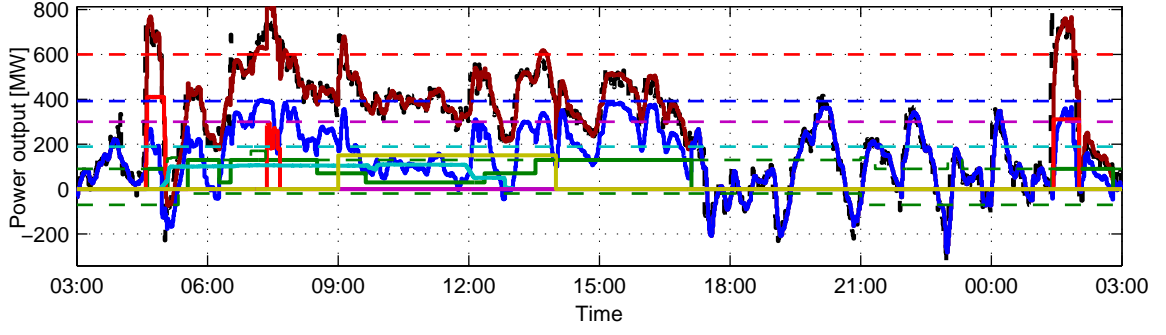
(a) Historical activation
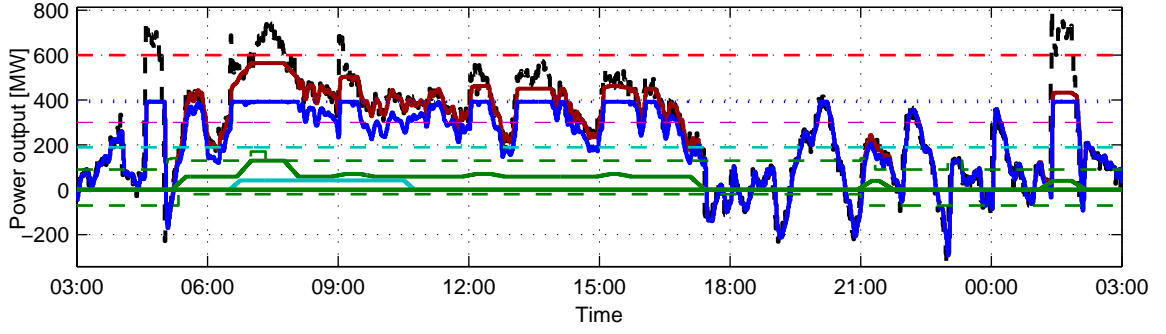
(b) Optimization result with penalization $C_{ACE}^{QP} = 20$
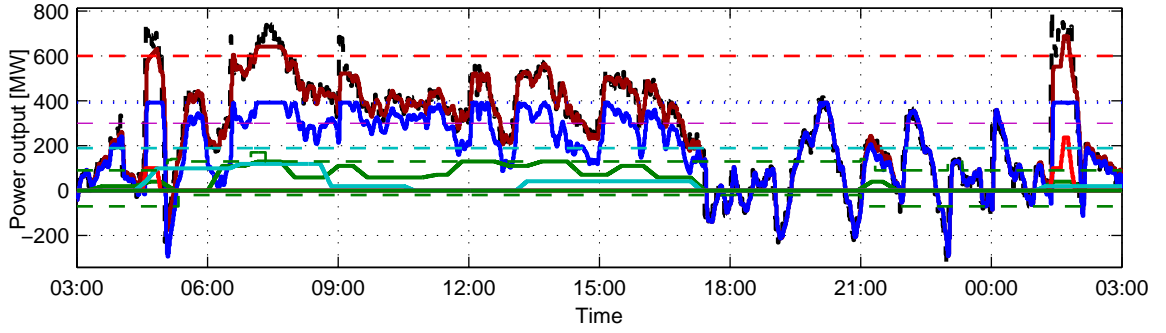
(c) Optimization result with penalization $C_{ACE}^{QP} = 40$
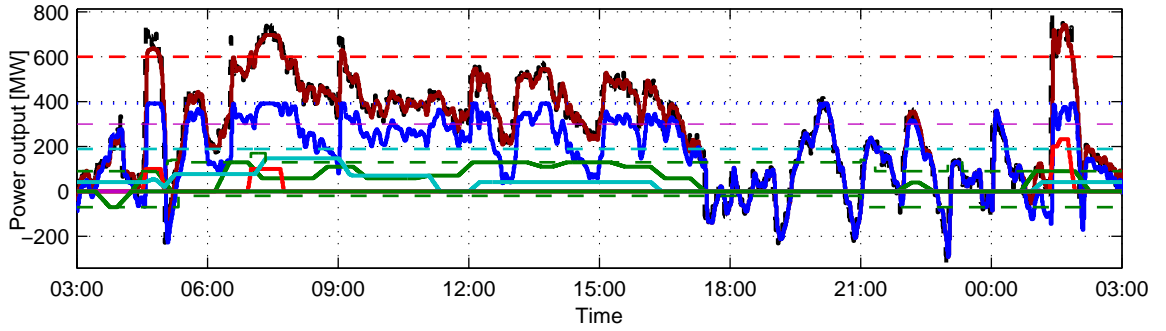
(d) Optimization result with penalization $C_{ACE}^{QP} = 60$
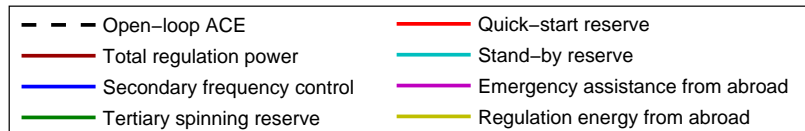
Figure 4.3: Example of the penalization C_{ACE}^{QP} influence

If the penalization coefficient is set to $C_{ACE}^{QP} = 20$, the controller tolerates relatively high values of closed-loop ACE in favour of not activating expensive regulation reserve units. As a result, the energy costs are reduced considerably, but the closed-loop ACE is 17% higher in comparison with historical activation. By increasing the penalization coefficient, the closed-loop ACE is reduced and the regulation energy costs rise. Low values of the penalization coefficient also reduce the frequency of unit activations and deactivations or power output changes, since small variations in open-loop ACE needn't be compensated. However, optimization speed with the quadratic form of the criterion is significantly lower compared to the linear form and due to the low solution time requirements, the linear form of the criterion was selected for the long term test case.

| | Relative regulation energy utilization [%] | | | | | | | | | ACE | Costs |
| | SR | | | TR | | | QS | SbR | RA | | |
	Tot.	SR$^+$	SR$^-$	Tot.	TR$^+$	TR$^-$					
History	55.1	51.5	3.6	17.4	17.4	0	6.0	10.9	10.6	100	100
$C_{ACE}^{QP} = 20$	84.6	81.0	3.6	12.8	12.8	0	0	2.6	-	117.2	67.7
$C_{ACE}^{QP} = 40$	72.4	68.6	3.8	16.1	16.1	0	1.5	10.0	-	92.1	79.0
$C_{ACE}^{QP} = 60$	66.6	62.4	4.2	17.4	16.9	0.5	3.0	13.0	-	86.3	84.1

Table 4.3: Penalization C_{ACE}^{QP} influence example - regulation energy utilization

4.1.4 Optimization results examples

The three 24-hour test cases shown in figures 4.4 to 4.6 were performed with two types of open-loop ACE prediction. The results denoted "real prediction" use the open-loop ACE predictor as described in [10]. The results denoted "ideal prediction" uses the resampled historical open-loop ACE as a prediction and therefore should remove prediction inaccuracy influence (but the influence of the time sampling of the optimization interval remains). For each test case, a table with regulation reserves distribution and closed-loop ACE and regulation energy costs comparison is included.

The first test case (figure 4.4) presents a situation with positive open-loop ACE higher than usual average, the second test case (figure 4.5) shows an opposite case with negative open-loop ACE higher than usual average and the third test case (figure 4.6) verifies the automatic controller performance on a typical situation in a power balance control,

without unusually high open-loop ACE.

For the first test case, the energy costs were reduced by approximately 20% with either of the two predictions in comparison with historical activation. However, since the sudden changes of the open-loop ACE, resulting for example from generation units outages, are difficult to predict, the open-loop ACE is 10% higher with the real prediction when compared to the ideal prediction. The schedule resulting from the optimization with the real prediction also shows increased secondary frequency control utilization, which was used to compensate the prediction error.

Similar conclusions may be made for the second test case with the real prediction - due to the prediction inaccuracy, larger volume of the secondary frequency control energy was utilized, resulting in significant decrease of energy costs, but also introducing situations, when open-loop ACE was not fully comensated. The energy costs in the result obtained based on the ideal prediction are higher, but the secondary frequency control is mostly kept within the reduced regulation range and thus increases the safety of the electric grid.

The cost reduction in the third test case is negligible when compared to the previous test cases. This stems from the fact that the regulation range of the secondary frequency control is high enough to compensate the open-loop ACE and the fact, that the energy price of the secondary frequency control is very low, hence little can be done to reduce the resulting energy costs.

To illustrate the effect of the prediction uncertainty, a part of the first test case schedule with uncompensated open-loop ACE is presented in figure 4.7 along with the step of the moving horizon optimization, which begins right before the time of the uncompensated open-loop ACE in the resulting schedule.

Several factors contributed to the final schedule - the CPC of the tertiary spinning reserve changed just before the start of the optimization horizon at 7:00 and therefore cannot be changed due to the CPC change limits, the stand-by reserve may not be activated immediately due to the activation delay and the secondary frequency control is already fully activated. Moreover, since the situation arose in the pumping time of the quick-start reserve units, the additional quick-start unit may only be activated to its maximal power output, which would have overcompensated the open-loop ACE prediction, so the quick-start reserve was not used either. As a result, no regulation reserve with sufficiently fast reaction time could be activated to compensate the open-loop ACE between 7:00 - 8:00.
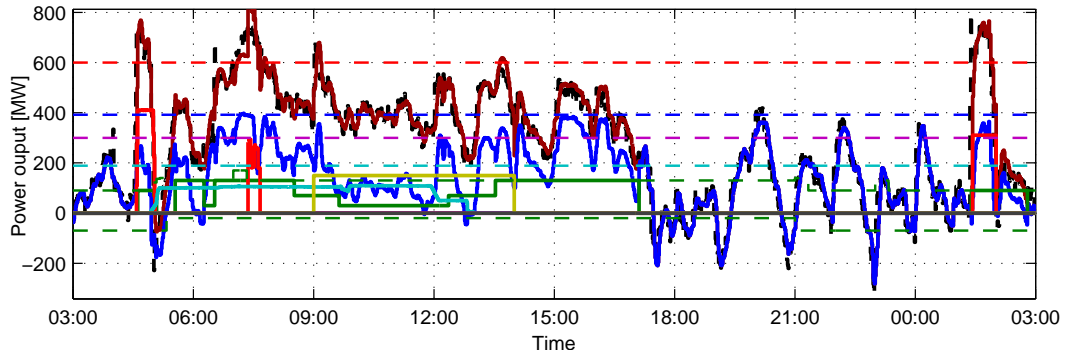
(a) Historical activation
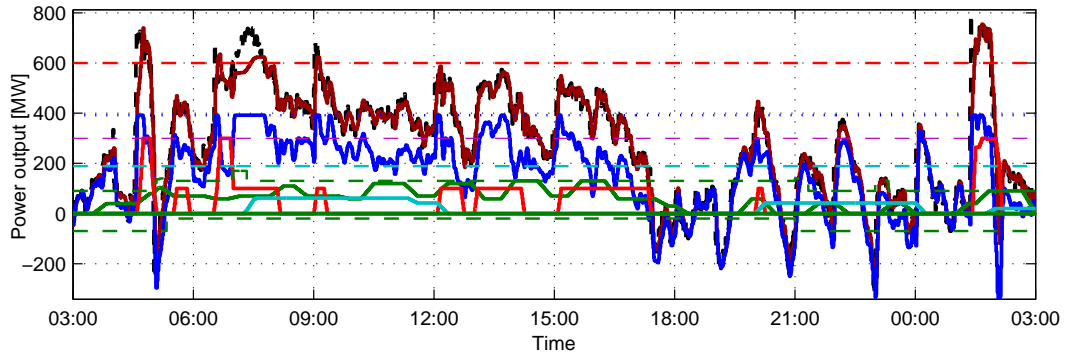
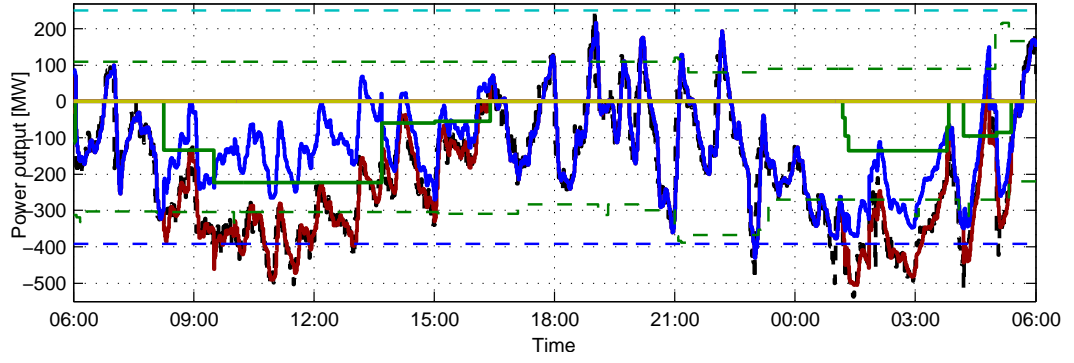(b) Optimization result with real prediction
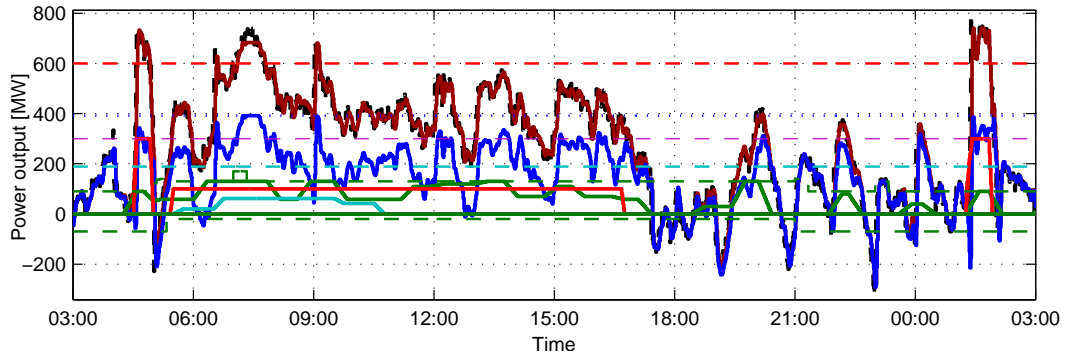
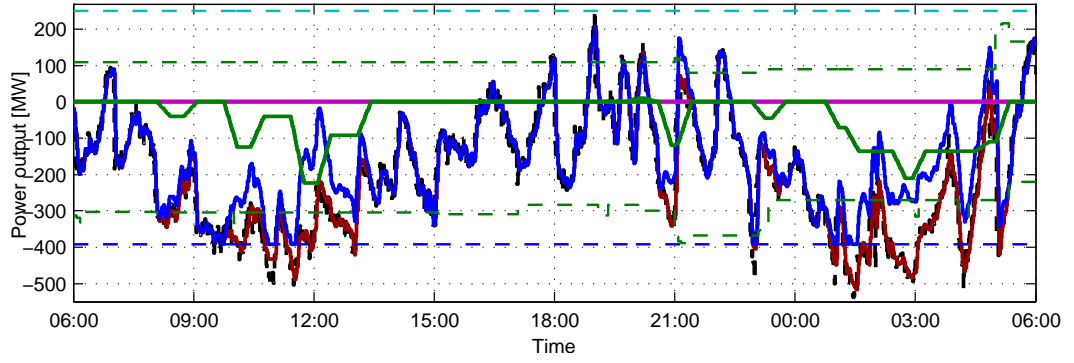(c) Optimization result with ideal prediction

Figure 4.4: Short term test case I

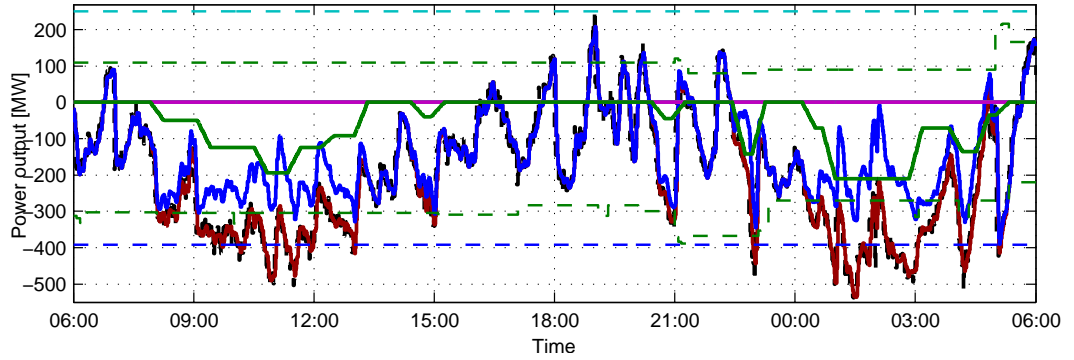|	Relative regulation energy utilization [%]									ACE	Costs
	SR			TR			QS	SbR	RA		
	Tot.	SR$^+$	SR$^-$	Tot.	TR$^+$	TR$^-$					
History	55.1	51.5	3.6	17.4	17.4	0	6.0	10.9	10.6	100	100
Real	60.9	55.3	5.6	19.1	19.1	0	13.5	6.5	-	95.8	80.5
Ideal	56.9	52.8	4.1	19.8	19.8	0	19.9	3.5	-	85.7	80.0

Table 4.4: Short term test case I - regulation energy utilization

(a) Historical activation

(b) Optimization result with real prediction

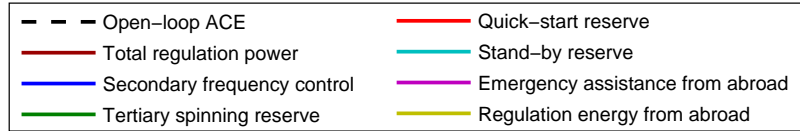(c) Optimization result with ideal prediction

Figure 4.5: Short term test case II

	Relative regulation energy utilization [%]								ACE	Costs
	SR			TR			QS	SbR		
	Tot.	SR$^+$	SR$^-$	Tot.	TR$^+$	TR$^-$				
History	67.2	4.8	62.4	32.8	0	32.8	0	0	100	100
Real	80.2	4.6	75.6	19.8	0.1	19.7	0	0	87.6	58.6
Ideal	73.9	4.0	69.9	26.1	0	26.1	0	0	85.1	70.9

Table 4.5: Short term test case II - regulation energy utilization

(a) Historical activation

(b) Optimization result with real prediction

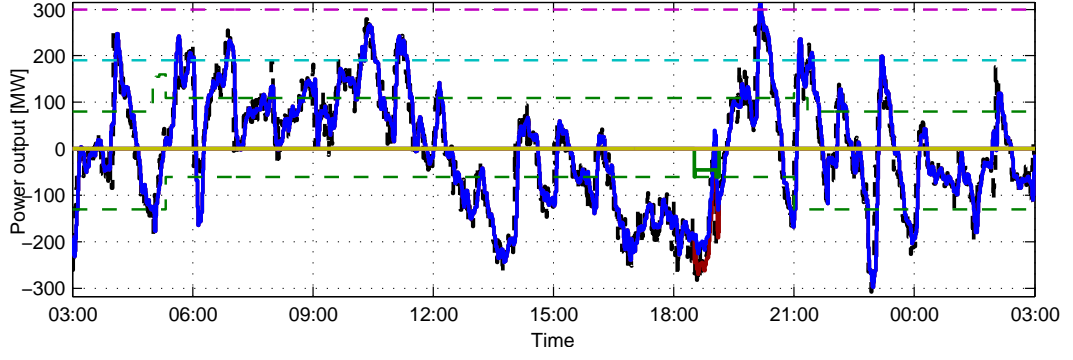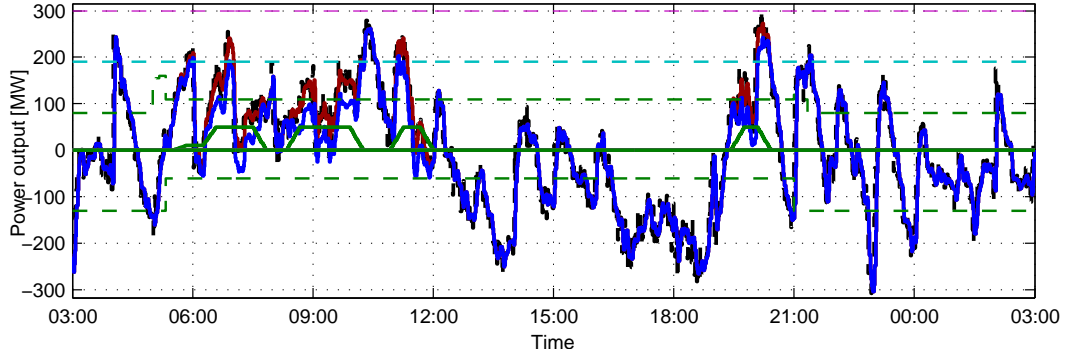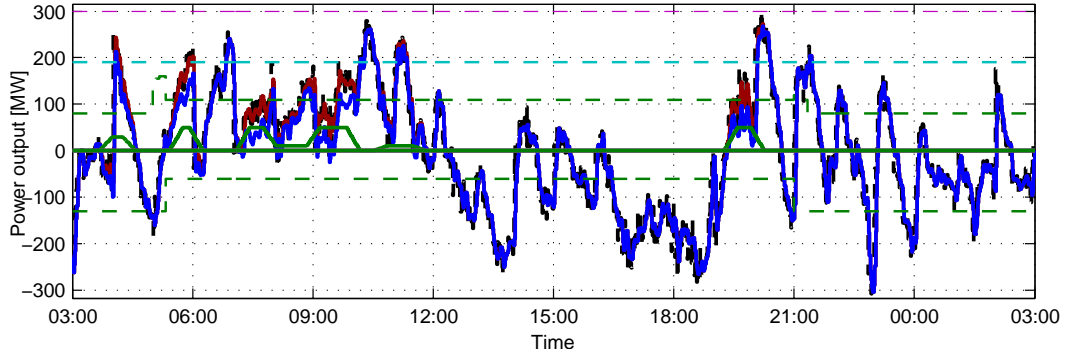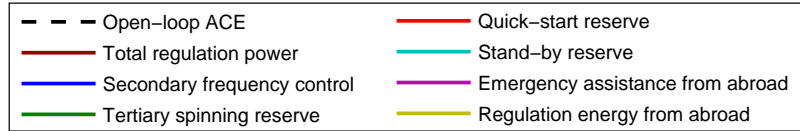(c) Optimization result with ideal prediction

Figure 4.6: Short term test case III

	Relative regulation energy utilization [%]								ACE	Costs
	SR			TR			QS	SbR		
	Tot.	SR$^+$	SR$^-$	Tot.	TR$^+$	TR$^-$				
History	98.9	48.9	50.0	1.2	0	1.2	0	0	100	100
Real	92.8	40.1	52.7	9.0	9.0	0	0	0	88.4	96.9
Ideal	93.6	41.3	52.3	7.4	7.4	0	0	0	88.5	96.0

Table 4.6: Short term test case III - regulation energy utilization
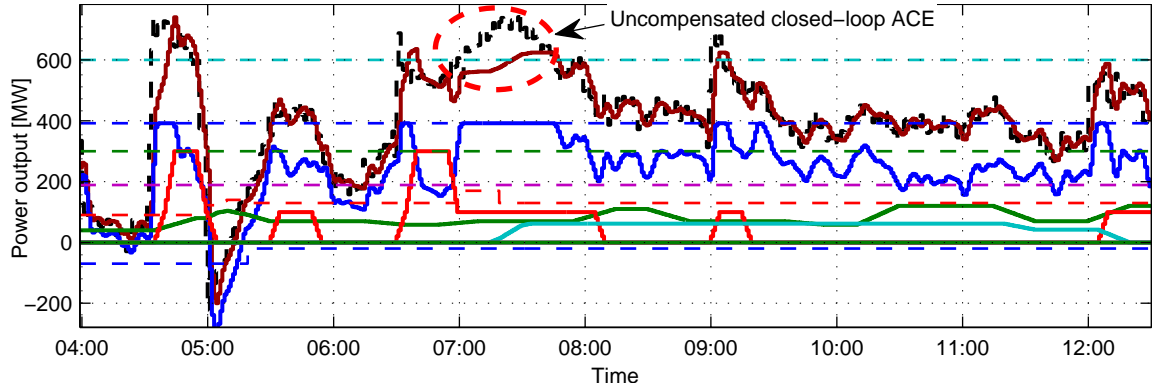
(a) Final schedule
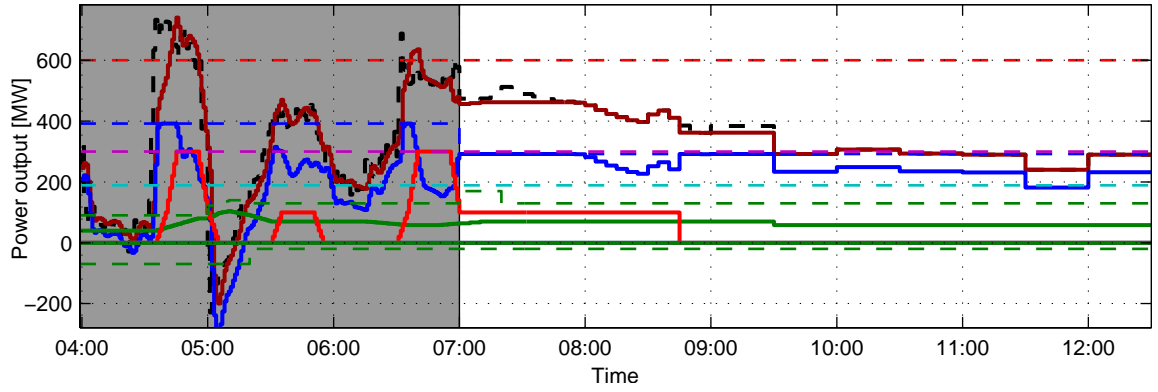
(b) A moving horizon step with prediction error

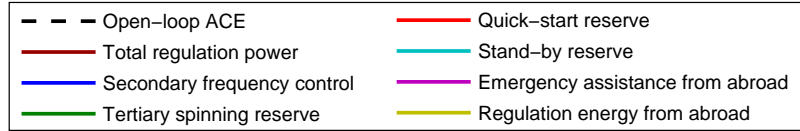|	
– – – Open–loop ACE	—— Quick–start reserve
—— Total regulation power	—— Stand–by reserve
—— Secondary frequency control	—— Emergency assistance from abroad
—— Tertiary spinning reserve	—— Regulation energy from abroad

Figure 4.7: Example of prediction inaccuracy influence

4.2   Long term performance evaluation

To gain more information on the automatic controller performance, a long term test on a one year interval was performed with both, the real and the ideal open-loop ACE prediction. The comparison of both results with the historical activation is presented in table 4.7.

The total costs were reduced by 7.8% in case of the real prediction and by 8% with the ideal prediction. As indicated in section 4.1.4, the energy cost reduction is mainly achieved in such situations, when the regulation range of the secondary frequency control

is insufficient to compensate the open-loop ACE alone and other regulation reserves must be activated. The resulting closed-loop ACE was lowered by 6.3% and 6.8% respectively, but such reduction may mainly be attributed to the differences in secondary frequency PI controller dynamics, as described in section 4.1.1.

	Comparison with the historical activation [%]										
	SR	SR$^+$	SR$^-$	TR	TR$^+$	TR$^-$	QS	SbR	ACE	Costs	RE
Real	100.5	98.3	102.1	147.2	160.0	117.2	82.5	43.7	93.7	92.2	99.8
Ideal	99.1	97.7	100.0	150.4	147.0	158.4	91.6	46.6	93.2	92.0	98.9

Table 4.7: Long term test case - comparison with the historical activation

	Relative regulation energy utilization [%]									
	SR	SR$^+$	SR$^-$	TR	TR$^+$	TR$^-$	QS	SbR	R$^+$	R$^-$
History	89.5	36.4	53.1	5.1	3.6	1.5	2.0	1.4	0.5	1.5
Real	90.2	35.9	54.3	7.5	5.7	1.8	1.7	0.6	-	-
Ideal	89.7	36.0	53.7	7.7	5.3	2.4	1.9	0.7	-	-

Table 4.8: Long term test case - regulation energy utilization

Generally more tertiary spinning reserve energy was used in comparison with the historical activation, mainly because it is more flexible than the stand-by reserve in terms of reaction time and activation change limits. This change may be observed in the tertiary spinning power output distribution histograms in figure 4.9, where the trend is most noticeable mainly in lower power outputs. Similarly, the increase of the low power output activations may be observed in the quick-start distribution in figure 4.10. The stand-by reserve power output distribution in optimization results (figures 4.11(b) and 4.11(c)) is more even across its regulation range when compared to the historical activation in figure 4.11(a).

The 1.4% difference in secondary frequency control energy volume between the result with the real and the ideal prediction means, that relatively large volume of regulation energy was substituted with more expensive regulation reserves in case of the ideal prediction in order to keep the safety margin. This stems from the fact, that the secondary frequency control energy forms around 90% of the utilized regulation energy as shown in table 4.8. Thus, the safety margin could be lower for optimizations with the ideal

prediction, which would result in reduction of energy costs. Such conclusion is also supported by the fact, that the number of situations when the power output of the secondary frequency control exceeded the safety margin is 60% higher in case of the real prediction when compared to the optimization result obtained with the ideal prediction.

When comparing the total volume of utilized regulation energy, the lower volume of the regulation energy and also lower resulting closed-loop ACE indicates that less counter-regulation (i. e. a state when both - positive and negative - regulation reserves are activated at the same time) was present in the case of the ideal prediction.
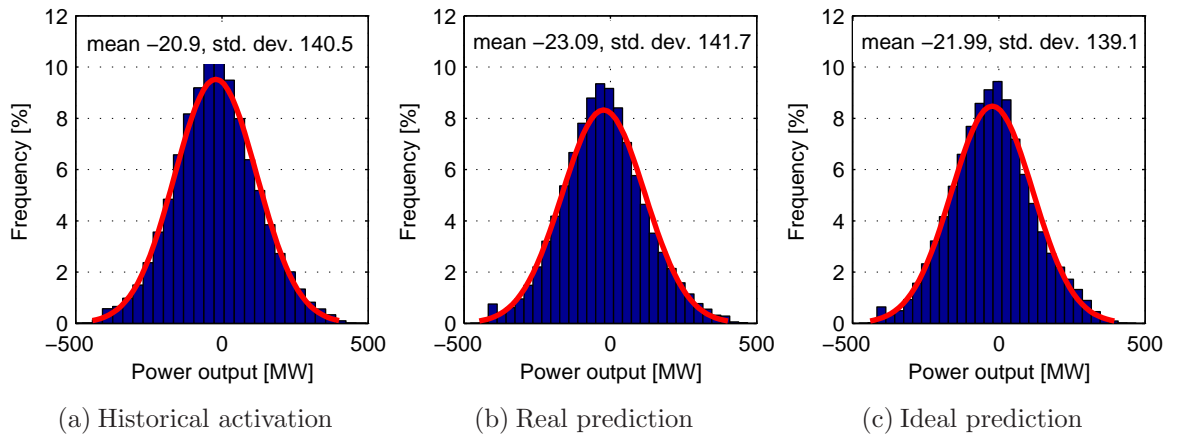

(a) Historical activation   (b) Real prediction   (c) Ideal prediction

Figure 4.8: Distribution of the secondary frequency control power output

(a) Historical activation   (b) Real prediction   (c) Ideal prediction
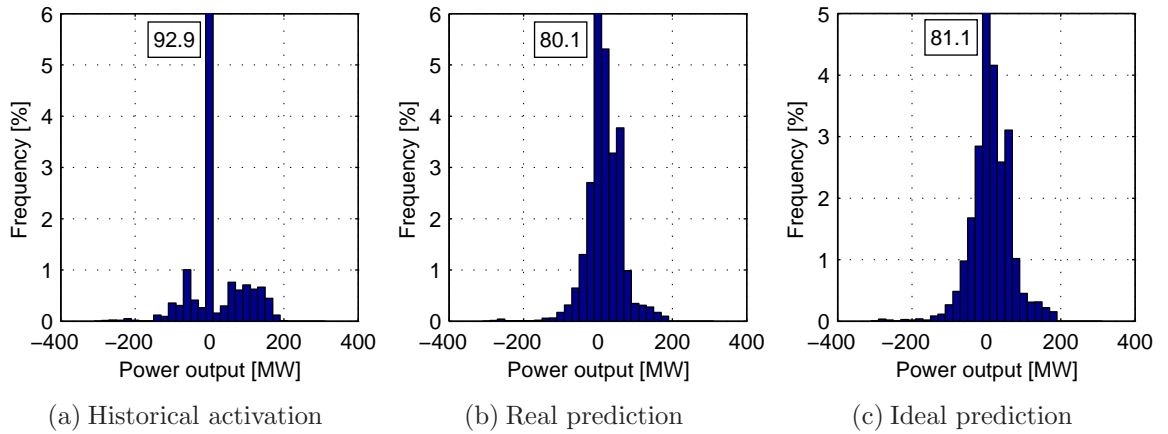
Figure 4.9: Distribution of the tertiary spinning reserve power output

(a) Historical activation   (b) Real prediction   (c) Ideal prediction
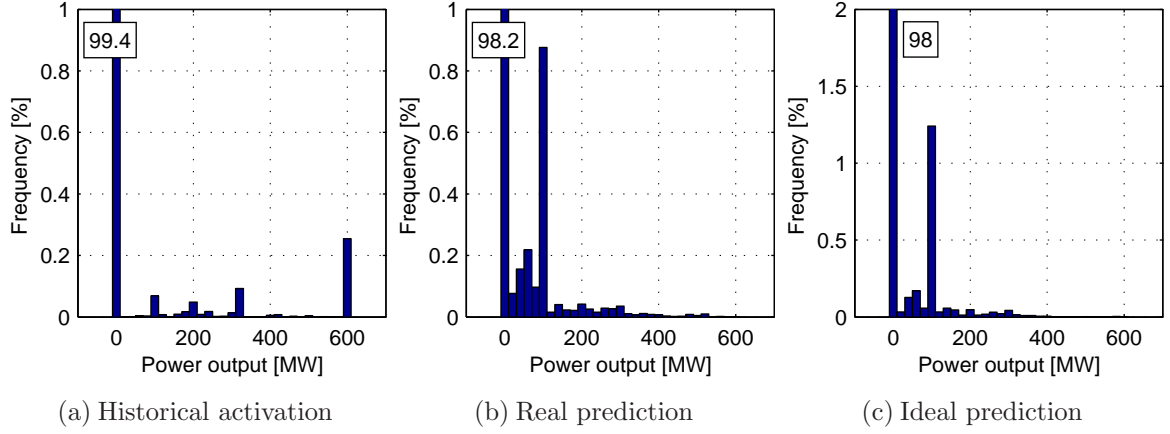
Figure 4.10: Distribution of the quick-start reserve power output

(a) Historical activation   (b) Real prediction   (c) Ideal prediction
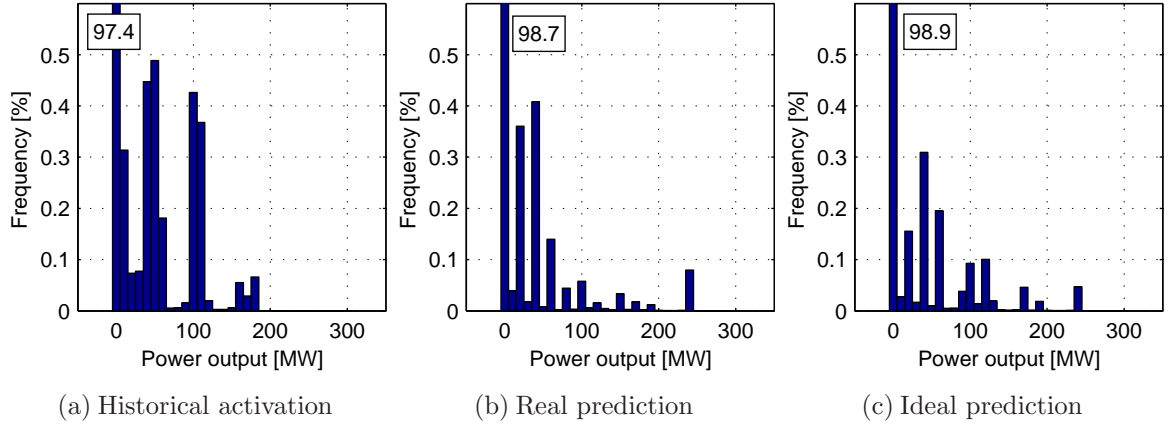
Figure 4.11: Distribution of the stand-by reserve power output

(a) Historical activation   (b) Real prediction   (c) Ideal prediction
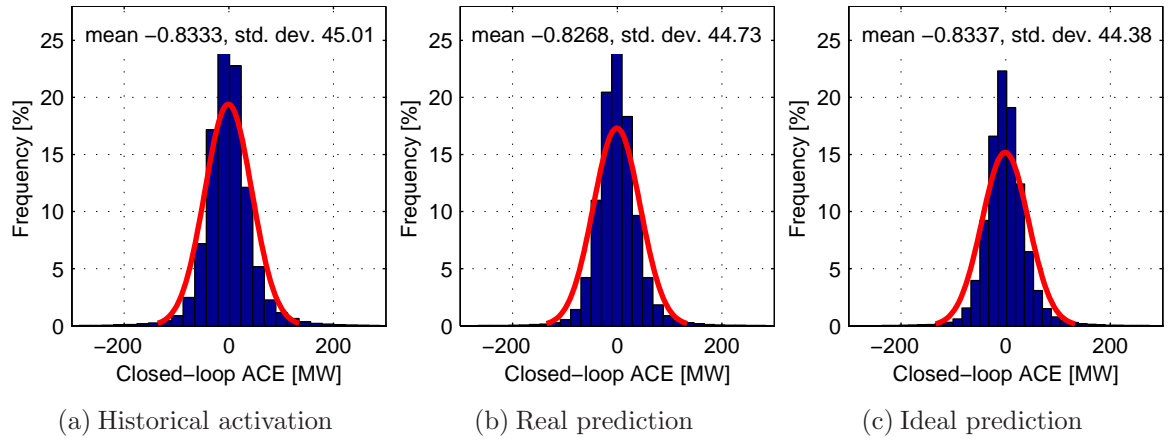
Figure 4.12: Distribution of the closed-loop ACE

4.3 Optimization speed evaluation

As the optimization speed is important to allow immediate application of the optimization results, the solution times during the long term test case computation were evaluated. The optimization was performed on a 2 x Intel Xeon E5420 at 4 x 2,5Ghz, 16 GB RAM machine and Windows 2008 Server 64-bit operating system. However, only single threaded version of CPLEX 11.0 was available, so the optimization could not take advantage of the multi-core setup. The resulting distribution of optimization times is shown in figure 4.13; more than 97% of all optimizations reached the optimality gap of 5%, which was set as a stopping criterion, in less than 20 seconds. In only 72 cases out of more than 200000 optimizations performed, the optimization failed to reach aforementioned optimality gap in a time limit of 300 seconds.
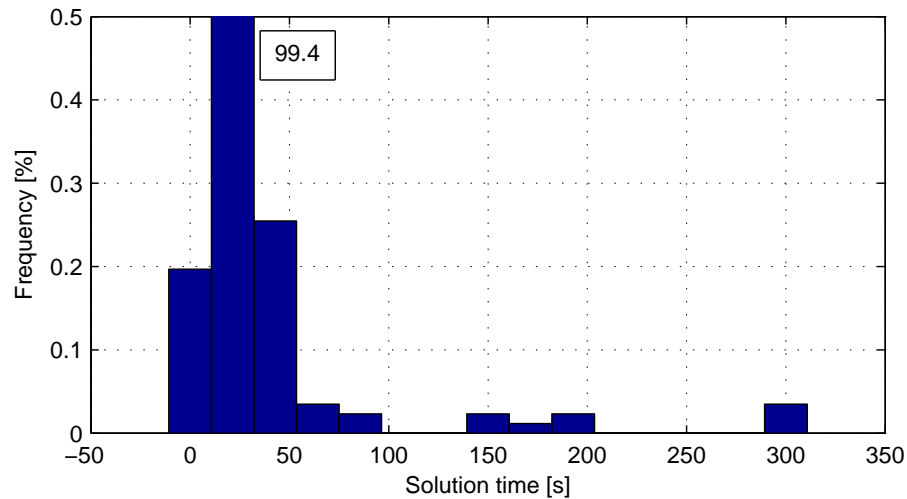
Figure 4.13: Distribution of the optimization times

Chapter 5

Conclusion

Three main goals have been set for this thesis - firstly, to modify the formulation of the cost-optimal dispatcher support system for power balance control in the transmission system, presented in [2], to better suit the needs of the Transmission System Operator dispatchers; secondly, to test the possibility of utilizing the system as an automatic power balance controller and finally, to test the system on realistic data.

The first goal was accomplished by formulating new models of regulation reserves dynamics and including dispatch constraints that allow to control the regulation reserves activation effectively. In comparison with the previous formulation, the new models are more precise and also include properties and other problem specifics not considered in the former formulation, such as variable maximal power output during the optimization horizon or activation of the tertiary reserve units in rising-price manner using the criterial price coefficient. The dispatch constraints, originally included in the optimality criterion as soft constraints, were transformed into hard constraints. As a result, the recent optimality criterion only contains the regulation energy costs and the control performance penalization, thus emphasizes the cost-optimality of the solution. Moreover, the new dispatch constraints have more straightforward interpretation and simplify the problem configuration.

The second goal was satisfied by transforming the dispatch system into a cost-optimal automatic controller by running the optimization on a moving horizon. This involves a correct transfer of initial conditions between the consecutive moving horizon steps to correctly implement the regulation reserves dynamics and the dispatch constraints. The operation in conjunction with the existing secondary frequency PI controller is simulated by employing the secondary frequency PI controller model to compute the secondary frequency control actions.

To fulfill the third goal, the automatic controller performance was evaluated in series of short and long term test cases and compared with the historical human-based control. It has proved to be capable of reducing the regulation energy cost while maintaining the required control performance. The quadratic form of the control performance penalization was analyzed as a way to allow for fine balancing of the regulation energy costs and the control performance, but due to lower optimization speed in comparison with the linear form, the linear form was selected for the long term tests.

The results of the optimization speed analysis, which was performed in the long term test case indicate, that for the most part, a satisfactory result was found in a time, which would allow a real-world controller application, especially as a decision support tool for the Transmission System Operator dispatchers.

In a future work, more test cases on historical data will be performed and the problem formulation will be rewritten in a standard modeling language, which would allow to make it independent on the Matlab environment and speed up the constraint generation process.

The main ideas of this thesis are also presented in paper [11], which is currently in submission process to the 7th IEEE International Conference on Control & Automation (ICCA'09), Christchurch, New Zealand.

References

[1] UCTE Operation Handbook, v2.2/20.07.04 (2004), [online]. ⟨http://www.ucte.org/_library/ohb/policy1_v22.pdf⟩.

[2] Malík, O. Predictive control of power balance in electric grid. Bachelor thesis. Czech Technical University in Prague, 2007.

[3] ČEPS, a.s. Praha. Kodex přenosové soustavy [online]. ⟨Revision 09, January 2009, http://www.ceps.cz/doc/kodex/revize09.zip⟩.
An english extract from the revision 09 of the Grid Code is available at ⟨http://www.ceps.cz/doc/kodex/part_I_II_III_an_rev09.pdf⟩.

[4] J. Löfberg. Yalmip : A toolbox for modeling and optimization in MATLAB. In *Proceedings of the CACSD Conference*, Taipei, Taiwan, 2004.

[5] The MathWorks MATLAB Website, 2009, [online]. ⟨http://www.mathworks.com/products/matlab/⟩.

[6] Bertsimas, D. and Tsitsiklis, J. N. *Introduction to Linear Optimization*. Athena Scientific, 1997.

[7] Ferrari-Trecate, G., Gallestey, E., Letizia, P., Spedicato, M., Morari, M, and Antoine, M. Modeling and Control of Co-Generation Power Plants: A Hybrid System Approach. In *IEEE Transactions on Control Systems Technology*, volume 12, No.5, pages 694–705, 2004.

[8] The ILOG CPLEX Website, 2009, [online]. ⟨http://ilog.com/products/cplex/⟩.

[9] Kalný, P. Simulační dynamický model provozu elektrizační přenosové soustavy. (in Czech). Diploma thesis. University of West Bohemia, Plzeň, 2007.

[10] Janeček, E., Janeček, P., Fialová, A., and Houdová, L. System deviation predictor (in Czech). Research report. University of West Bohemia, Plzeň, 2008.

[11] HAVEL, P. and MALÍK, O. Optimal Dispatch of Regulation Reserves for Power Balance Control in Transmission System. In submission process to the 7th IEEE International Conference on Control & Automation (ICCA'09), Christchurch, New Zealand, 2009.

Appendix A

Contents of the included CD

The included CD contains an electronic version of this diploma thesis.